1-1-2017

Synthesis and Light-Harvesting Potential of Cyanovinyl β-Substituted Porphyrins and Dyads

Rhys Mitchell
University of Wollongong, rtm442@uowmail.edu.au

Klaudia K. Wagner
University of Wollongong, kwagner@uow.edu.au

Jonathan E. Barnsley
University of Otago

Holly van der Salm
University of Otago

Keith C. Gordon
University of Otago, kgordon@chemistry.otago.ac.nz

See next page for additional authors

Synthesis and Light-Harvesting Potential of Cyanovinyl β-Substituted Porphyrins and Dyads

Abstract

Knoevenagel condensation has been utilized as an alternative way to synthesize a series of β-vinyl-substituted porphyrins and porphyrin dyads with good to excellent yields. The condensation of β-formyl porphyrins and phenylacetonitriles allows control of the substitution pattern and metal centres in the porphyrin dyads, allowing the use of metallated synthons. While the optical and electronic properties of the resulting porphyrin dyes are perturbed by the presence of the cyano substituent, this does not significantly affect their use. For example, Raman spectroscopy, in agreement with density functional theory (DFT) and time-dependent DFT (TD-DFT) calculations, show porphyrin electronic transitions with delocalization of frontier molecular orbital electron density onto the β substituent. A comparison of the photovoltaic performance of a carboxylated cyanostyryl condensation product and the unsubstituted analogue in dye-sensitized solar cells (DSSCs) was made. Although the devices showed similar efficiency, the device containing the cyano-substituted dye showed an extended incident photon-to-current conversion efficiency (IPCE) due to a slight red-shift in absorption and an increase in photovoltage as a result of a longer electron lifetime. This minimal change in light-harvesting performance highlights the potential of this Knoevenagel synthetic methodology for producing light-harvesting porphyrin dyes.

Disciplines

Engineering | Physical Sciences and Mathematics

Publication Details

Mitchell, R., Wagner, K., Barnsley, J. E., van der Salm, H., Gordon, K. C., Officer, D. L. & Wagner, P. (2017). Synthesis and Light-Harvesting Potential of Cyanovinyl β-Substituted Porphyrins and Dyads. European Journal of Organic Chemistry, 2017 (38), 5750-5762.

Authors

Rhys Mitchell, Klaudia K. Wagner, Jonathan E. Barnsley, Holly van der Salm, Keith C. Gordon, David L. Officer, and Pawel W. Wagner

FULL PAPER

Synthesis and Light Harvesting Potential of Cyanovinyl β-Substituted Porphyrins and Dyads

Rhys Mitchell,[a] Klaudia Wagner,[a] Jonathan Barnsley,[b] Holly van der Salm,[b] Keith C. Gordon,[b] David L. Officer*[a] and Pawel Wagner*[a]

Abstract: Knoevenagel condensation has been utilized as an alternative way to synthesize a series of β-vinyl substituted porphyrins and porphyrin dyads with good to excellent yields. The condensation of β-formyl porphyrins and phenylacetonitriles allows control of the substitution pattern and metal centres in the porphyrin dyads, allowing the use of metallated synthons. While the optical and electronic properties of the resulting porphyrin dyes are perturbed by the presence of the cyano substituent, this does not significantly affect their use. For example, Raman spectroscopy, in agreement with DFT and TD-DFT calculations, show typical porphyrin electronic transitions with delocalisation of frontier molecular orbital electron density onto the β-substituent. A comparison of the photovoltaic performance of a carboxylated cyanostyryl condensation product and the unsubstituted analogue in dye sensitised solar cells was made. Although the devices showed similar efficiency, the device containing the cyano-substituted dye showed an extended IPCE due to a slight red-shift in absorption and an increase in photovoltage as a result of a longer electron lifetime. This minimal change in light harvesting performance highlights the potential of this Knoevenagel synthetic methodology for producing light harvesting porphyrin dyes.

Introduction

Over recent years, synthetic porphyrins have proved to be outstanding light harvesting materials whether as part of antenna systems, on surfaces or for solar cells.[1] One of the key challenges in using them as light harvesting materials is to extend the porphyrin energy absorption of readily prepared synthetic porphyrins across the visible spectrum as much as possible. As has been well documented, the electronic properties of porphyrins can be altered by chemical functionalisation and the attachment of a conjugated system has the ability to extend the porphyrin energy absorption.[2] For example, the β-pyrrolic modification and extension of the porphyrin π-system significantly broadens and red shifts the light absorption.[3] In particular, electron withdrawing substituents have the ability to move electronic absorption toward the red,[4] and, as a result of the improved light harvesting, increase the performance of dye sensitised solar cells (DSSCs).[5] A variety of chemistries have been used to extend the conjugation of either single porphyrins or multiporphyrin arrays. Suzuki, Heck and Wittig reactions have all been used to extend porphyrin conjugation through the β-pyrrolic position by introduction of a vinyl group.[6] The first two processes have poor selectivity toward mono-substituted porphyrins as mono-borylation and bromination of the porphyrin core is low yielding and results in difficult purification.[5a, 7] Those problems can be overcome by the use of Wittig chemistry.[8]

With the ready availability of either the β-pyrrolic porphyrin aldehydes or methylphosphonium salts, we and others have used Wittig chemistry to produce a variety of vinyl linked functionalised porphyrins and porphyrin arrays.[8-9] The reactions are moderate to high yielding and tolerant of a variety of functionalities and metals. Nonetheless, challenges with this type of synthesis remain including the production of *E, Z* isomeric mixtures, the problematic isolation of the desired products from unwanted side products such as methylporphyrins, and the sometimes difficult formation of unsymmetrical or multimetallated porphyrin arrays.[8] New synthetic methodology is needed to address these challenges, particularly in the latter case. To this end, Knoevenagel chemistry appears as an interesting alternative. Analogous to the Wittig chemistry, β-formylporphyrins could provide the building blocks for the formation of both conjugated single porphyrins by initial reaction with phenylacetonitriles as well as porphyrin dyads through subsequent reactions with the initially formed porphyrinylacetonitriles (Route b, Scheme 1). Conversely, a single condensation of the appropriate phenyldiacetonitrile could provide a symmetrical dyad (Route a, Scheme 1). Larger arrays could also be fabricated using the appropriately substituted phenylacetonitriles.

Therefore, in this study we demonstrate the simple synthesis of a series of modified porphyrins by Knoevenagel condensation between β-pyrrolic formylporphyrins and a series of phenylacetonitriles. Symmetrical and unsymmetrical porphyrin dyads have also been synthesised. Electrochemistry and Raman spectroscopy show the effects of the electron withdrawing phenylacetonitrile. We also demonstrate that this facile synthesis can provide a porphyrin modified with a carboxylic acid that can be successfully used as a light harvesting dye in a DSSC.

[a] R. Mitchell, K. Wagner, D. L. Officer, P. Wagner
ARC Centre of Excellence for Electromaterials Science and Intelligent Polymer Research Institute
AIIM Faculty
University of Wollongong
Northfields Avenue
Wollongong, NSW 2522, Australia
E-mail: davido@uow.edu.au and pawel@uow.edu.au
[b] J. Barnsley, H. van der Salm, K. C. Gordon,
Department of Chemistry
University of Otago
Dunedin, New Zealand

Supporting information for this article is given via a link at the end of the document.

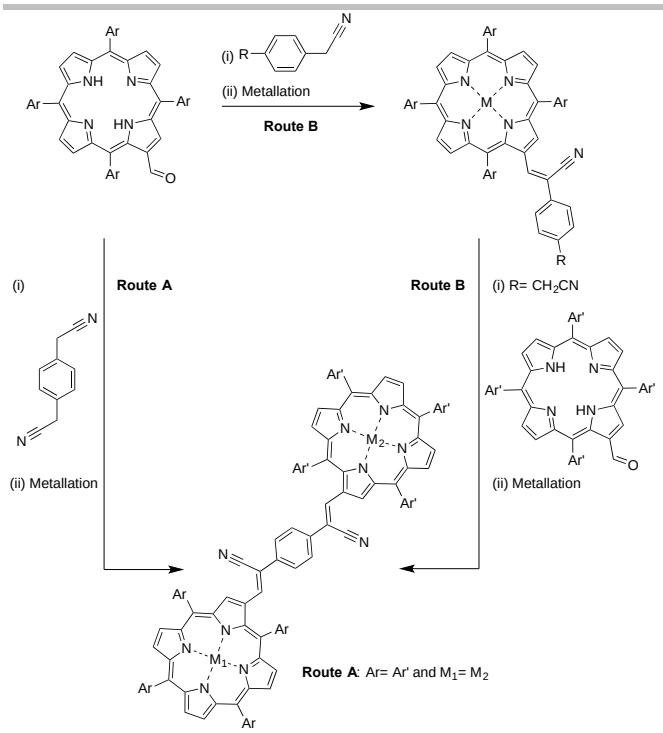

Scheme 1. General Knoevenagel condensation routes for synthesis of functionalised porphyrins and porphyrin dyads.

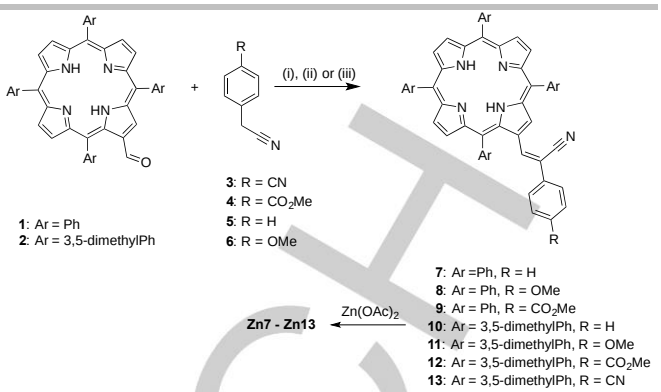

Porphyrin	Method	Yield (%)
7	(i)	80
8	(i)	84
9	(i)	84
10	(ii)	37
11	(ii)	37
12	(iii)	59
13	(iii)	57

Scheme 2. Synthesis of functionalised porphyrins **Zn7**- **Zn13**. Reaction conditions: (i) DBU, CH_2Cl_2, RT. (ii) DBU, 1,2-dichloroethane, microwave (100°C). (iii) KOtBu, DMF, microwave (100°C).

Results and Discussion

Synthesis of Vinyl β-Substituted Porphyrins

Porphyrin β-pyrrolic aldehydes **1** and **2** react with phenylacetonitriles **3** and **4** at room temperature using 1,8-diazabicycloundec-7-ene (DBU) as a base to form porphyrin derivatives **9**, **12** and **13** in 84%, 93% and 80% yield, respectively (Scheme 2). The electron rich phenylacetonitriles **5** and **6** failed to react under these conditions. Heating of porphyrin aldehydes **1** and **2** with **5** and DBU by microwave irradiation provided **7** and **10** in 37% yield. The presence of the strong electron donating methoxy group in **6** suppressed the reaction such that a stronger base, potassium *tert*-butoxide (KOtBu), had to be used. Under those conditions (stronger base and microwave irradiation), products **8** and **11** were then obtained in 59% and 57% yield, respectively. Zinc insertion into the vinyl porphyrins was performed according to standard techniques and gave **Zn7**-**Zn13** in quantitative yields.[10]

The reactivity of the phenylacetonitriles is strongly influenced by the substitution pattern of the benzene ring. While electron deficient phenylacetonitriles, which facilitate carbanion formation, react under mild conditions, electron-donating substituents tend to suppress the process requiring harsher conditions such as higher temperature or/and use of stronger base. However, the microwave conditions also produced uncharacterised baseline material, which resulted in generally lower yields. The substituents on the porphyrin aldehydes had little impact on the outcome of the reactions.

^{1}H NMR spectroscopy provides evidence for a change in electronics of the modified porphyrins. The ^{1}H NMR spectra of the CN styryl porphyrins **7-13** all show similar chemical shifts characteristic of these types of molecules, with the key difference being the influence of the cyano group both electronically and through space on its neighbouring protons.[10] Thus, compared to the previously reported styryl-substituted porphyrins, the introduction of the cyano group results in a downfield shift of the β-pyrrolic proton H_3. For example, comparison of methoxy derivative **8** and the non-cyano substituted derivative shows a shift of β-pyrrolic proton H_3 from 9.05 ppm to 9.48 ppm.[11] Clearly, the neighbouring cyano group deshields this proton with the remaining 6 β-pyrrolic protons uninfluenced. The ^{1}H NMR spectrum of **8** also contains a single pyrrolic NH peak and a simplified aromatic region.

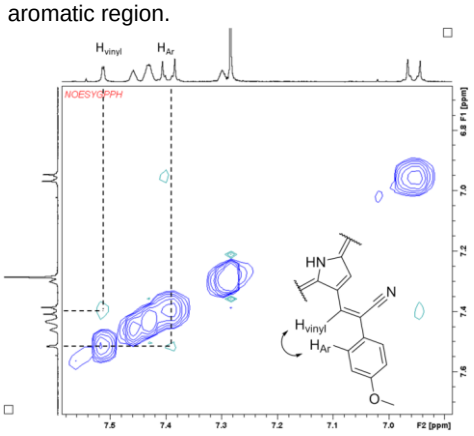

Figure 1. NOESY spectrum of **8** showing coupling between H_{vinyl} and H_{Ar}.

During condensation with non-symmetrical CH acids, two possible isomers *E* and *Z* can be formed. However, in the case of these CN styryl compounds, only one isomer is formed in contrast

to previously studied Wittig reactions.[11] The NOESY NMR technique was necessary to determine the configuration of the synthesised isomer. The NOESY spectrum showed coupling between H_{vinyl} and H_{Ar}, which is indicative of the Z isomer. The E isomer does not have this spatial orientation, as H_{vinyl} is not in the proximity of H_{Ar} (Figure 1).

Synthesis of Porphyrin Dyads

As indicated in Scheme 1, porphyrin dyads can be made either using a single step (Route A) or two steps (Route B). The attempt to synthesize a symmetrical porphyrin dyad by reacting 2 equivalents of 2-formylporphyrin **14** with 1 equivalent of 1,4-phenylenediacetonitrile **15** with DBU in chloroform gave dyad **16** in a very low yield (12%) (Scheme 3). This synthesis was repeated using various conditions, however a difficult to separate mixture of unreacted aldehyde **14**, a mono-adduct and dyad **16** was obtained in all cases. Yields were not improved by microwave irradiation or by increasing the equivalents of porphyrin aldehyde **14** to 1,4-phenylenediacetonitrile **15** (4:1 and 10:1).

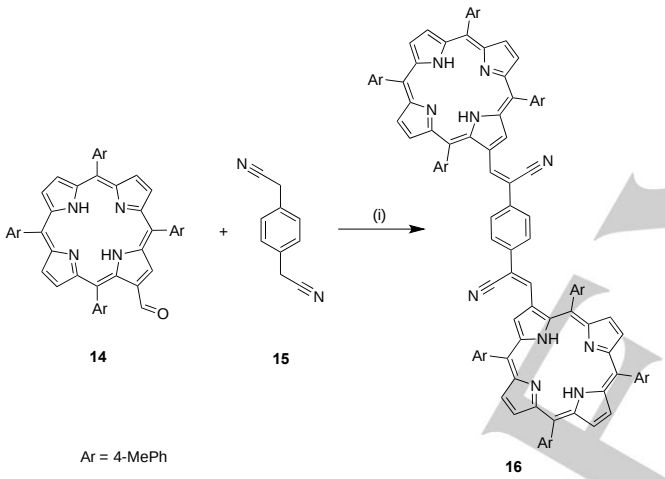

Scheme 3. One step synthesis of porphyrin dyad **16**. Reaction conditions: (i) DBU, $CHCl_3$, reflux.

Consequently, a two-step approach that could also provide a synthetic route to non-symmetrical porphyrin dyads containing different porphyrins or different metal centres was investigated.[10] Mono adducts of a series of porphyrins were initially prepared in the first step by reaction of formylporphyrins **1**, **2**, **17** with 1,4-phenylenediacetonitrile **15** (Scheme 4). Microwave irradiation was required to maximise the reaction products. Best results were observed by reacting the 2-formylporphyrin with 10 equivalents of 1,4-phenylenediacetonitrile **15** and a large excess DBU in 1,2-dichloroethane. The reactions were heated at 100 °C at 250 W for 30 min in a microwave reactor. Porphyrins **18**-**20** were obtained in moderate to good yields after purification. Conventional reflux, or the use of a stronger base such as KOtBu, did not drive the reaction to completion, with formylporphyrin starting material consistently observed.

The successful syntheses of cyano compounds **18**-**20** provided precursors for the preparation of a series of asymmetric and variably metallated porphyrin dyads. The 4-ethylphenylstyrylporphyrin derivative **20** was reacted with 2.5 equivalent of tetraxylylporphyrin aldehyde **2** using microwave irradiation (250 W, 120 deg, 30 min) with complete consumption of **20** and a resulting isolated yield of the asymmetric dyad **21** of 80% (Scheme 4). The excess of aldehyde was necessary to drive the reaction to completion. Attempts to reduce the amount of aldehyde and simultaneously increasing the reaction time were unsuccessful due to apparent increased decomposition. The full conversion of the starting material **20** was essential, as the post-reaction purification of the mixture of **20** and dyad **21** proved to be problematic.

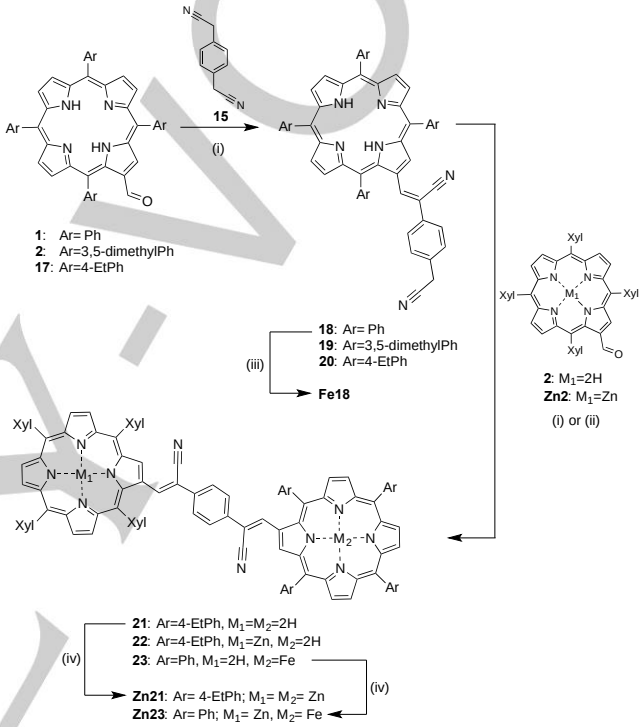

Porphyrin	Method	Yield (%)
18	(i)	80
19	(i)	78
20	(i)	68
21	(i)	80
22	(ii)	70
23	(i)	45

Scheme 4. Synthesis of porphyrin dyads. Reaction conditions: (i) DBU, 1,2-dichloroethane, microwave. (ii) NaOMe, 1,2-dichloroethane, microwave. (iii) $FeCl_2$, acetonitrile, reflux, followed by exposure to O_2. (iv) $Zn(OAc)_2$, CH_2Cl_2, MeOH, RT.

The structure of dyad **21** was readily confirmed using NMR spectroscopy and mass spectrometry. Two sets of NH proton signals are evident in the 1H NMR spectrum along with two distinct singlets due to the β-pyrrolic protons adjacent to the vinyl substituents on each porphyrin.

During synthesis of dyad **22** from styrylporphyrin **20** and aldehyde **Zn2**, two products were obtained. Upon purification, an inseparable mixture of the free base-zinc (II) and free base-free base dyad was obtained. Control experiments under the same microwave conditions used in the Knoevenagal synthesis with zinc 5,10,15,20-tetraphenylporphyrin (**ZnTPP**) in DCE, DCE and

DBU, and DCE and H_2O showed that the zinc was only retained in the porphyrin core when using DCE. Therefore, it appears that water in a reaction mixture is able to remove zinc under these conditions; given the hydroscopic nature of DBU, it is not surprising that zinc was removed from dyad **22**. Replacement of DBU with sodium methoxide consequently allowed the synthesis of **22** without demetallation, with the dyad being formed in 70% yield after 60 min (Scheme **4**).

The spectral characteristics of dyad **22** were very similar to that of the free base dyad **21** albeit with the absence of one pyrrollic proton signal due to the insertion of zinc and one vinyl singlet apparent at 7.80 ppm.

Synthesis of the free base-Fe (III) porphyrin dyad **23** was achieved by reaction of **Fe18** and formyl porphyrin **2** with DBU as base under microwave conditions with a shortened reaction time in a moderate yield (45%). Zinc insertion was achieved according to standard conditions to produce **Zn21** and **Zn23**.[10]

The UV-visible and mass spectral data were consistent with the formation of the dyads.

Electrochemical Analysis

Electrochemical analysis of the single cyano styrylporphyrins **Zn7 - Zn9** showed (Table 1 and Figure 2), as expected, the presence of four reversible processes: two oxidations and two reductions.[12]

Table 1. E/V *vs*. $Fc/Fc^{+\cdot}$ for **Zn7 - Zn9** and **Zn24** in CH_2Cl_2.

	$E_{1/2}$			
Compound	Oxidation		Reduction	
Zn7	0.33	0.60	-1.65	-1.90
Zn8	0.31	0.59	-1.68	-1.93
Zn9	0.33	0.62	-1.58	-1.82
Zn24	0.29	0.55	-1.79	-2.05

Comparison of one of these cyano substituted porphyrins **Zn7** to the analogous cyano-free styrylporphyrin **Zn24** (Table 1 and Figure 2a) shows that there is little difference in oxidation potentials, with the major effect of the nitrile group being on the reduction potentials; the introduction of the electron withdrawing group shifts electron density from the porphyrin core, resulting in positive shifts of the reduction potentials by 140-150 mV.[11]

The reduction potentials of the cyanostyrylporphyrins are also affected by the substituents on the benzene ring (Table 1). With reference to **Zn7** (Ph derivative), the electron withdrawing ester group on **Zn9** shifts both reduction potentials more positively by 70-80 mV. The introduction of the electron donating methoxy group on **Zn8** has less of an effect, and shifts the reduction potentials by 30 mV toward negative values (Figure 2b). Therefore, the introduction of the electron withdrawing cyano group has a significant effect on the reduction potentials of the porphyrin ring, with the aromatic group substituents less influential on the porphyrin electronics.

a)

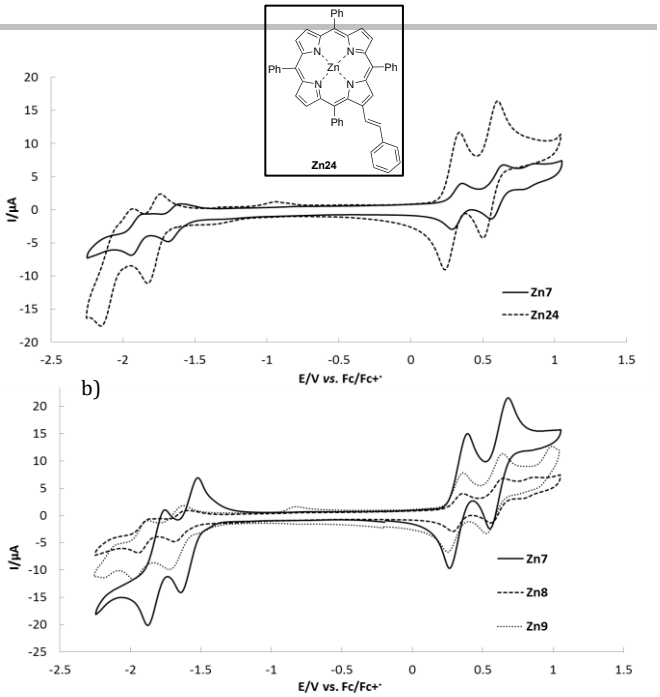

Figure 2. a) Cyclic voltammograms of **Zn7** in comparison to **Zn24** in CH_2Cl_2. b) Cyclic voltammograms of **Zn7**, **Zn8** and **Zn9** in CH_2Cl_2. Scan rate 50 mV s^{-1}.

UV-visible Spectroscopy

The ultraviolet-visible (UV-vis) spectra of the cyano styryl-appended porphyrins and dyads are similar to those previously reported for this type of phenylene-linked porphyrin. As reported by Burrell *et al.* for the analogous symmetrical free base phenylene-linked dyads,[13] the dyad spectra observed are linear combinations of their constituent porphyrin monomers albeit with a strong shoulder present on the low-energy side of the Soret band at ~ 490 nm that leads to a broadening of the Soret band, as can be seen in Figure S1 for Zn free base dyad **22.** This shoulder and the related band broadening has been attributed to the beginning of a split Soret band as a result of limited electronic coupling between the two porphyrins of the dyad; dyads with strong coupling such as those with acetylene or butadiyne bridges have two Soret bands due to splitting.[14]

In contrast, the Q bands are largely unaffected. Analogous to the single tetraarylporphyrins (TAPs) and zinc TAP starting materials, the free base dyads show four Q bands and the metallated compounds only two as a result of the porphyrin *D*2h (TAPs) and *D*4h (zinc TAP) symmetries.[15]

Raman Spectroscopy and DFT Calculations

Of interest here is the role and degree to which the CN group affects the styryl substituent and the CN and OCH_3 aryl functionalization electronically tune the β-aryl substituent and the porphyrin core. Species **Zn10, Zn11** and **Zn13** offer such comparisons and allow for some comparison with the literature in order to determine the effect of CN substitution on the styryl functionality.[11] All compounds exhibit similar spectra with strong Raman bands between 1500 and 1580 cm^{-1} (Figures S2 and 3). A number of small spectral variances are observed between compounds, most of which occur in this high energy region. The

strong coupling of typical porphyrin vibrations (ν(Cb–Cb), ν(Pyr. half-ring) and ν(Pyr. breathing)) to β-substituent vibrations indicate an intimately connected electronic system is present.

Bands at 1579, 1566, 1524 and 1500 cm^{-1} for **Zn13** (Figure 3), for example, show vibrational contribution from the β-substituent and yield the largest shifts and changes in intensity. This indicates a successful electronic tuning of the axillary β-substituent dependent on the electron withdrawing nature of the functional group (CN>H>OMe). The band at 1363 cm^{-1}, known as the ν_4 band, which is often used as a spectroscopic marker for the metalloporphyrin core size, shows little change between compounds, but is blue-shifted when compared to unsubstituted ZnTPP (1356 cm^{-1}).[16] The steric torsion induced by β-substitution is known to cause deformation of the porphyrin structure (ruffled, saddled, domed or waved) and can be monitored through shifts of the ν_4 band.[16] Such spectral variations indicate both electronic and geometric tuning by the β-substituted unit. Analogous spectra for **Zn10** and **Zn11** can be found in Figure S2.

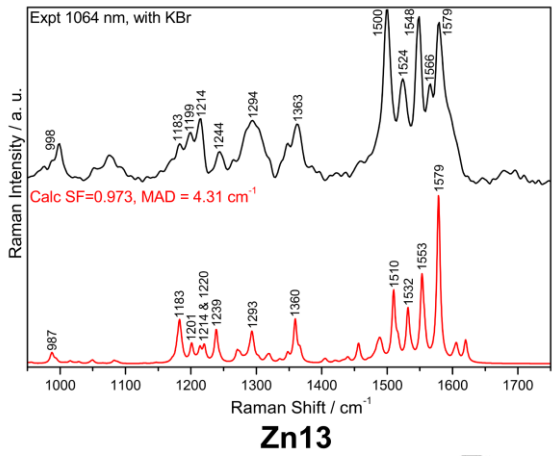

Figure 3. Experimental FT-Raman (black) and DFT calculated frequency (red) spectra of **Zn13**. The experimental spectrum was obtained at 1064 nm using a KBr pellet.

To investigate structural deformation, density functional theory (DFT) analysis was carried. FT-Raman data was used as a verification method for DFT ground state geometries by comparing experimental and calculated Raman spectra to generate a mean absolute deviation (MAD).[17] MADs for the three compounds investigated are sufficiently small (<6 cm^{-1}) which indicates an effective model of the structure has been achieved. Tabulated Raman peaks can be found in Table S1 with DFT assisted assignments.

Optimised ground state geometries for **Zn10**, **Zn11** and **Zn13** exhibit saddling distortions with pyrrole-pyrrole angles of ~13° and are shown in Figure S3. A slight increase in saddling is noted for the phenyl derivative **Zn10**. Such distortion results in a predicted mean N-Zn bond-length of 2.072 Å for all compounds, compared to a ZnTPP mean of 2.066 Å. These results are consistent with a blue-shifted ν_4 band.

Bond length variation (Figure S4) from ZnTPP is observed mostly within the β-substituent pyrrole ring; with elongations of bond 2 and 3 and a shortening of bond 4 (atoms 2-3, 3-4 and 4-5 respectively). Similar patterns are observed for all three compounds, indicating a likeness of the bonding network. Deformation of these bonds is supportive for variation of the ν (Pyr. half-ring) based ν_4 band observed in experimental FT-Raman data. These variations are predicted to be no more than 2.5 pm, which represents small disparities.

Distortion of the porphyrin core is well documented to cause a breakdown of the Gouterman four orbital model, consequential for the physical and optical properties.[18] Figure S5 details frontier molecular orbitals for the compounds of interest and ZnTPP with the energetics of these orbitals summarised in Figure 4. Typical a_{1u}, a_{2u} and e_g (HOMO-1, HOMO, LUMO and LUMO+1) orbitals are observed for ZnTPP. For **Zn10**, **Zn11** and **Zn13** orbitals HOMO-1, HOMO and LUMO+1 remain mostly unperturbed while HOMO-2, LUMO and LUMO+2 exhibit electron density on the β-substituent, especially so for HOMO-2. With β-substitution, a splitting of the e_g set occurs, narrowing the band gap, while a_{1u} and a_{2u} become more energetically disparate.

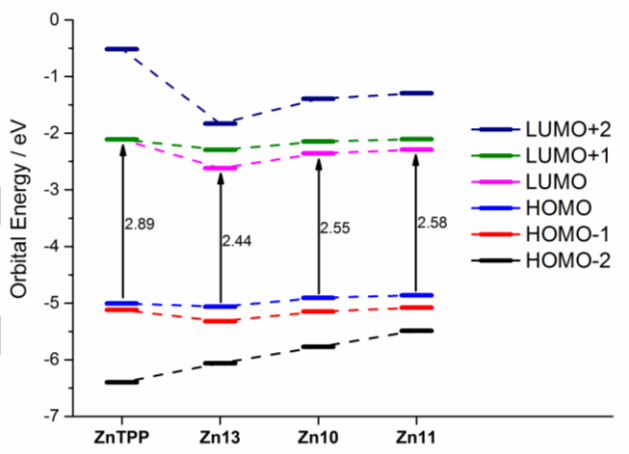

Figure 4. DFT generated frontier molecular orbital energies.

TD-DFT allows the prediction of UV-Visible absorption and results are shown in Table S2. TD-DFT provides a prediction of experimental results to 0.1 eV. Orbitals from H-2 to L+2 are involved in both Q and B band transitions. Q transitions terminate sufficiently on LUMO and L+2 orbitals resulting in a partial donation to the β-substituent of +22% for **Zn13**, +10% for **Zn10** while **Zn11** is predicted to donate -5%, indicating electron density shifting to the porphyrin. For the strong B band, +18, +10 and -29% donation to the β-substituent is observed for **Zn13**, **Zn10** and **Zn11** respectively. These results indicate the decrease of electron withdrawing as a result of CN, H and OMe functionalization, and are consistent with FT-Raman data.

Q:B intensity ratios have been generated and are displayed in Table S3. The less degenerate $^1(a_{2u}e_g)$ and $^1(a_{1u}e_g)$ configurations, the weaker the Q band and hence the smaller the Q:B ratio.[4b] For this reason, Q:B ratios provide an indicator of geometric and electronic distortion. In both experimental and calculated data, there is an increase of the Q:B ratio on β-substitution, with the largest values observed for **Zn13**.[19] The energy gap between Q and B bands decreases with β-substitution, with the smallest experimental gap also predicted for **Zn13**.

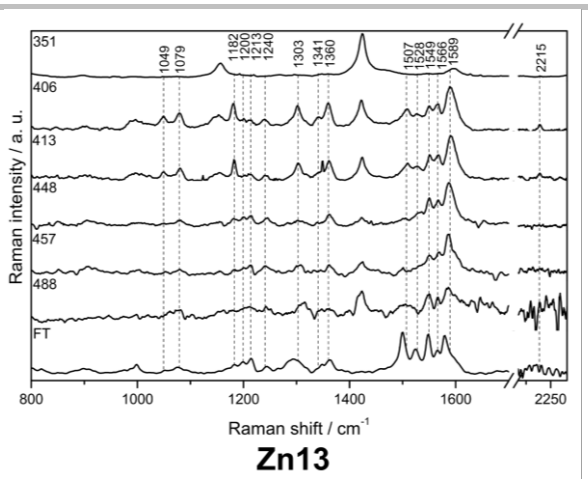

Figure 5. Resonance Raman spectra of **Zn13** in CH_2Cl_2 with a range of excitation wavelengths across the Soret band.

Resonance Raman provides a method of identifying active chromophoric regions within molecules as a result of region specific vibrational enhancement that occurs coincident with ground → excited state distortions.[17] Spectra were collected across the Soret band region (emission precludes measurement in the Q band region) to investigate the origins of optical transitions for dyes **Zn13** (Figure 5), **Zn10** and **Zn11** (Figure S6). Strong porphyrin bands are present as expected, while the presence of bands at 1079, 1182 and 1240 also demonstrate the involvement of the β substituent at excitations of 406 and 413 nm. This pattern of enhancement is considerably changed from electronically separated porphyrins with β-substituents as seen by Earles *et al.*,[20] and indicates an effective communication between these units similar to that observed by Walsh *et al*.[3b] For **Zn13**, and **Zn11** there are slight differences in the 1500-1620 cm^{-1} pattern of band enhancement as the excitation wavelength is tuned to the B band; especially present at excitations of 406 and 413 nm. This result is consistent with TD-DFT calculations, which predict two transitions that involve different MOs but are generally similar in nature. Modes 1507 and 1589 cm^{-1} evolve beside the ground state bands 1500 and 1579 cm^{-1} indicating these bands are not equivalent. The origin of these bands is thought to be strongly β-substituent coupled vibrations that are minimally polarisable, however are resonantly enhanced due to β-substituent contribution to the B band. Phenyl derivative **Zn10**, which has no para substituent, shows only one pattern of band enhancement is present, indicative of a homogeneous transition in the Soret region.

Interestingly, in all resonance Raman data, the nitrile band (2215 cm^{-1}) is weak, when compared to a direct porphyrin β-bound nitrile group studied by van der Salm *et al*.[21] Hence, the contribution from the styryl nitrile group to the absorption properties is less. Vibrations associated with the appended phenyl group and ethene linker indicate that the β-substituent is electronically connected to the transitions, consistent with the TD-DFT analysis (Table S2).

In comparison to analogs lacking cyano-substitution at the styryl region, core size marker band ν4 (~1365 cm^{-1}) is red-shifted in these species (1360 cm^{-1}), while ν2 remains unchanged at ~1550 cm^{-1}. This indicates that despite a non-participation of the styryl CN unit for absorption; some structural effect is present from this region, likely in the form of electronic withdrawal. In support of this proposition, **Zn13**, **Zn10** and **Zn11** appear to lack the typical ~1620 cm^{-1} band associated with the C=C vibrational mode.[11, 21] DFT calculations indicate this band shifts to lower wavenumber and likely is obscured by band structure at 1590 cm^{-1}. The effect of CN substituents on $\nu(C=C)_{styryl}$ modes has been investigated in terthiophene systems and reflect a vibrational redshift of this band, similar to results presented here.[22]

Dye Sensitised Solar Cell Performance

For the study of the influence of the cyano group on the light harvesting characteristics of the porphyrin, a new cyano-substituted styryl-appended porphyrin carboxylic acid **Zn25** was prepared from the ester **Zn12** and compared in the dye sensitised solar cell (DSSC)[23] to the analogous cyano-free porphyrin acid **Zn26** (Figure 6) whose light harvesting characteristics have been well studied.[24] DSSCs were fabricated in a standard glass configuration with a 12 μm TiO_2 layer, platinized counter electrode and iodine electrolyte as described in the experimental section.

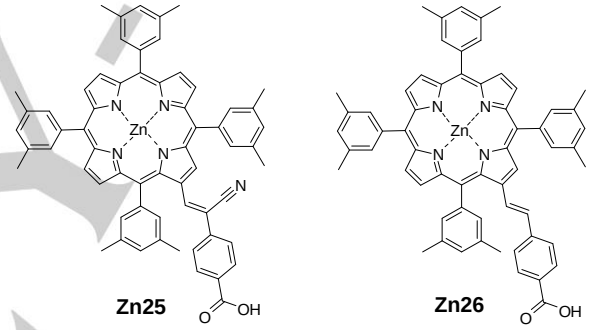

Figure 6. Structure of porphyrin **Zn25** and previously synthesised **Zn26**.[24]

The sensitisation of TiO_2 was performed in tetrahydrofuran (THF) solution and the UV/Vis spectra of **Zn25** and **Zn26** in THF and adsorbed on TiO_2 are shown in Figure 7. In the solution spectrum of **Zn25,** the Soret band at 428 nm has a significant shoulder 446 nm (Figure 7a), which indicates formation of aggregates.[25] Both the TiO_2 spectra (Figure 7b) show a significant broadening of the Soret band, again indicative of both H and J aggregates on the semiconductor surface with the cyanoporphyrin **Zn25** showing a slightly more broadened Soret band.

Table 2. Photovoltaic characteristics of **Zn25** and **Zn26** sensitised DSSCs.*

Dye	V_{oc} [mV]	J_{sc} [mA/cm^2]	FF	η [%]
Zn25	630	7.05	0.70	3.11
Zn26	608	7.12	0.71	3.07

*The data is obtained from an average of 3 devices.

A summary of the photovoltaic results obtained from the DSSCs with **Zn25** and **Zn26** on 12 μm TiO_2 films is presented in Table 2. The photovoltage observed for the DSSC sensitised with **Zn25** is higher than that of **Zn26** although the observed photocurrent for the **Zn25** device is slightly lower. With equivalent FFs, the final photovoltaic efficiencies are almost identical (3.1 %).

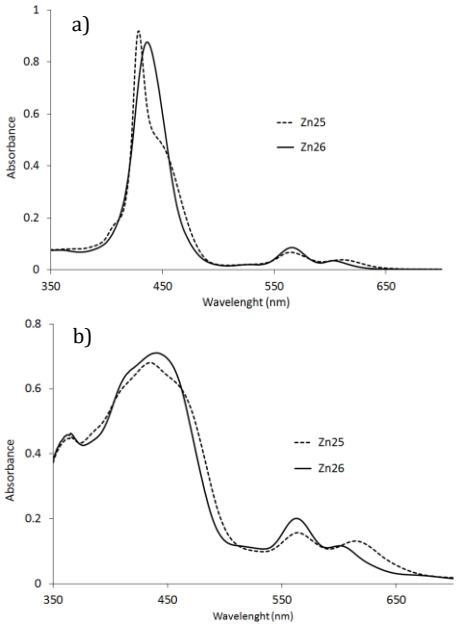

Figure 7. UV–vis absorption spectra of **Zn25** and **Zn26** in THF (a) and on TiO_2 (b).

Figure 8 shows the incident photon-to-current efficiencies (IPCEs) of both porphyrin-sensitized solar cells. While **Zn26** has a larger IPCE across the entire absorption spectrum, **Zn25** has a broader light harvesting range, although this is not sufficent to, provide the same amount of current, corresponding to an observed higher J_{sc} for **Zn26**. In addition, as shown in Table 1 for other cyanostyrylporphyrins, the first reduction potential of a cyanostyrylporphyrin is significantly more positive than the analogous non-cyano styrylporphyrin (140 mV for **Zn7** vs **Zn24**). Thus, the LUMO of cyanostyrylporphyrin **Zn25** would be expected to be lower than that of the non-cyano porphyrin **Zn26**, resulting in a smaller driving force and potentially less current.

Devices containing **Zn25** and **Zn26** were further investigated by electrochemical impedance spectroscopy performed at V_{oc} conditions and 1 sun light exposure. Nyquist and Bode plots are shown in Figure S7.

To gain a better insight into electron recombination (V_{oc}) in the investigated cells, the electron lifetimes were estimated from the Bode plots. The calculated values of electron lifetimes for **Zn25** and **Zn26** were 3.2 and 2.5 ms, respectively (see SI). The longer electron lifetime for **Zn25** corresponds to the higher V_{oc} observed for these devices.

While the UV-vis spectra of **Zn25** and **Zn26** on TiO_2 (Figure 7b) suggested that a comparable amount of dye was absorbed, a dye uptake measurement from the TiO_2 sensitized photoanodes was carried out. However, as shown in Figure S8, aggregation of the resulting tetrabutylammonium salt of **Zn25** prevented accurate quantification of the dye uptake. Nonetheless, as has been shown, the photocurrent of the two dyes is similar supporting the presence of the same amount of dye on the TiO_2 surface.

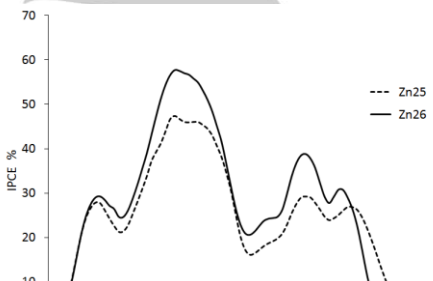

Figure 8. Incident photon-to-current conversion efficiencies (IPCEs) for both porphyrins: **Zn25** and **Zn26**.

Conclusions

Knoevenagel chemistry has been utilised to provide a series of functionalised porphyrins and porphyrin dyads with moderate to excellent yields. We have established by NMR analysis that the products were present as only the *Z* isomer. Porphyrin dyads were also prepared by Knoevenagel chemistry, with porphyrin geometry and metalation state being controlled in the step-by-step synthesis.

Electrochemical analysis shows the incorporation of the electron withdrawing cyano group into the porphyrin side chains is able to shift electron density off the porphyrin core in relation to their Wittig-linked counterparts. Electrochemical analysis also indicated that the aromatic substituent on the side chain benzene ring is able to affect reduction of the porphyrin, although the cyano group remains the dominant influence.

Raman data, in concert with DFT and TD-DFT calculations, shows little difference in structure between **Zn10**, **Zn11** and **Zn13**. Spectroscopy indicates that the Soret band electronic transitions resemble normal porphyrin transitions, simply with some delocalisation of frontier molecular orbital electron density onto the β substituent.

The effect on light harvesting and electron injection by the cyano substitution was also examined by fabricating DSSCs. The introduction of the side chain cyano group into a light harvesting porphyrin dye **Zn25** shows slightly higher photovoltage but lower photocurrent when compared to the cyano-free analog **Zn26**. The IPCE spectrum demonstrated broader light harvesting by **Zn25** (red shift about 25 nm) but less current measured. This is rationalised on the basis of lower driving force as a result of the electronwithdrawing character of the cyano group depleting the electron density of the π conjugated system of the porphyrin and lowering the HOMO.

Impedance spectroscopy supported the higher V_{oc} for **Zn25** sensitized devices through longer electron lifetimes. The higher resistance of the dye/TIO_2/electrolyte interface for **Zn25** is likely a consequence of less efficient electron injection. Nonetheless, the effect of the cyano functionality on the dye performance was minimal, demonstrating the value of this simpler and more efficient Knoevenagel method for the production of these types of conjugated dyes.

Experimental Section

Materials: All reagents, solvents and compounds **3**, **4**, **5**, **6** and **15** were obtained from commercial sources and used without further purification. Aldehydes **1**, **2** and **14** were synthesized via Vilsmeyer formylation as described previously.[9a] The synthesis of **Zn24** and **Zn26** were performed according to literature procedures.[11, 24] Flash chromatography used silica, 40-60µm with the indicated solvents.

Spectroscopy: Electronic absorption spectra were obtained using a Shimadzu UV-1800 spectrophotometer,.

Proton (^{1}H) nuclear magnetic resonance (NMR) spectra were obtained at 400 MHz using a Bruker Ultrashield 400 Plus spectrometer. ^{1}H NMR data is expressed in ppm, with all peaks shifted in reference to tetramethylsilane as the internal standard.

Electrochemistry: Electrochemical experiments were performed in a three-electrode cell with a glassy carbon working electrode, a platinum mesh as the counter electrode, and Ag|AgCl (leakless) as the reference electrode. All potentials are reported against the apparent formal potential of the ferrocene/ferrocenium couple. The cyclic voltammograms (CVs) of compounds were obtained at 1 mM in degassed CH_2Cl_2 with 100 mM tetrabutylammonium perchlorate present. Cyclic voltammetry (CV) measurements were performed using a CHI 76D electrochemical analyzer (CH instrument, CHI650D). All electrochemical experiments were performed at room temperature (23 ± 2 °C) in air.

Raman Spectroscopy: FT-Raman spectra were recorded on solid-state KBr disks using a Bruker MultiRAM instrument with 1064 nm excitation wavelength and a liquid nitrogen cooled D418T Germanium detector controlled by OPUS v7.2 software. Spectral resolution was 4 cm^{-1}, power used was 15 mW and typically 256 scans were co-added.

Resonance Raman spectra were recorded with the excitation beam focussed onto the sample with an obtuse-angle backscattering geometry. The scattered photons were collected with a plano-convex lens and focussed onto the entrance slit of an Acton Research SpectraPro500i spectrograph with an aperture-matched lens. Laser radiation was rejected before the slit using long-pass filters (Semrock Inc.). The beam was horizontally dispersed with a 1200 grooves mm^{-1} grating onto a liquid-nitrogen cooled Spec10:100B CCD, which was controlled using WinSpec/32 software (Roper Scientific) and calibrated with a 1:1 v/v toluene:acetonitrile mixture. Wavelengths 350.7, 406.7 and 413.1 nm were provided by an Innova I-302 krypton ion laser (Coherent Inc.), 448 nm was provided by a diode laser (CrystaLaser), and 457.9 and 488.0 nm were provided by an Innova Sabre argon ion laser (Coherent Inc.).

Calculations: Gaussian09 was used to optimise structures with a B3LYP functional and 6-31G(d) basis set, both in vacuo and in a solvent field (PCM model). Frequency and TD-DFT calculations used the same parameters. The mean absolute deviation between experimental and simulated non-resonant Raman spectra was used to validate the calculations.

DSSC Fabrication: Two investigated porphyrins were tested in a standard, glass configuration dye sensitized solar cells with iodine/iodide electrolyte.. TiO_2 photoanodes were prepared on fluorine-doped tin oxide (FTO) substrates (Hartford Glass, $R_s \leq 7$ Ω sq^{-1}) using a screen printing technique with commercially available paste. A blocking layer and $TiCl_4$ treatment were employed. The thickness of the TiO_2 layer was 12 µm (one layer screen printed 43T mesh transparent Dyesol paste (DSL 18NR-T) and one layer scattering Dysol paste WER2-0).

The active areas of films were 0.16 cm^2 (4 x 4 mm). Films were sintered stepwise using a programmable hotplate with a maximum temperature of 500°C. TiO_2 films at 110°C were immersed into 0.2 mM solution of **Zn25** or **Zn26** in tetrahydrofuran (THF) for 2 h. Sandwich-type DSSCs were assembled using a 25 µm Hymilan sealant and thermally platinized counter electrode on FTO (Hartford Glass, $R_s \leq 7$ Ω sq^{-1}). The electrolyte solution, composed of 0.6 M DMPII, 0.5 M 4-*tert*-butylpyridine, 0.1 M LiI and 0.05 M I_2 in a solvent mixture of 85:15 acetonitrile/valeronitrile, was injected into the inter-electrode spacing through a hole in the counter electrode, which was subsequently sealed.

Functionalised Porphyrin Monomers

7

In a 10-mL microwave reaction vial, a solution of 2-formyl-5,10,15,20-tetraphenylporphyrin **1** (30 mg, 47 µmol), phenylacetonitrile **5** (30 mg, 0.27 mmol), DBU (0.7 mL) in 1,2-dichloroethane (1.0 mL). The reaction was heated at 110 ^{0}C, power 250 W for 50 min under microwave irradiation. The cooled reaction was then purified by flash chromatography (silica, CH_2Cl_2) and crystallisation from CH_2Cl_2/MeOH, to give the desired product **7** (13 mg, 37%) as a purple-brown solid. ^{1}H-NMR (400 MHz, $CDCl_3$): δ 9.49 (s, 1H, $H_{β\text{-pyrrolic}}$), 8.94 (d, 1H, ^{3}J= 5.0 Hz, $H_{β\text{-pyrrolic}}$), 8.87 (d, 1H, ^{3}J= 5.0 Hz, $H_{β\text{-pyrrolic}}$), 8.83-8.76 (m, 3H, $H_{β\text{-pyrrolic}}$), 8.72 (d, 1H, ^{3}J= 5.0 Hz, $H_{β\text{-pyrrolic}}$), 8.32-8.27 (m, 2H, $H_{o\text{-Ar}}$), 8.24-8.17 (m, 6H, $H_{o\text{-Ar}}$), 7.84-7.66 (m, 12H, $H_{m,p\text{-Ar}}$), 7.61 (d, 1H, ^{4}J= 1.2 Hz, H_{vinyl}), 7.40-7.35 (m, 5H, H_{AR}), -2.59 (br s, 2H, NH). UV-vis (CH_2Cl_2) $λ_{max}$ (log ε) 428 (5.26), 523 (4.22), 561 (3.85), 599 (3.78), 658 (3.57) nm. HRMS, *m/z*: calcd for MH^+ ($C_{53}H_{35}N_5$): 742.2971, found: 742.3005.

8

A solution of 2-formyl-5,10,15,20-tetraphenylporphyrin **1** (60 mg, 93 µmol), 4-methoxyphenylacetonitrile **6** (82 mg, 0.56 mmol), KOtBu (100 mg) in DMF (2.1 mL) was heated to 100 ^{0}C, 250 W for 20 min in a microwave reactor. The cooled reaction was then purified by flash chromatography (silica, CH_2Cl_2) and crystallisation from CH_2Cl_2/MeOH, to give the desired product **8** (41 mg, 57%) as a purple-brown solid. ^{1}H-NMR (400 MHz, $CDCl_3$): δ 9.45 (s, 1H, $H_{β\text{-pyrrolic}}$), 8.93 (d, 1H, ^{3}J= 5.0 Hz, $H_{β\text{-pyrrolic}}$), 8.86 (d, 1H, ^{3}J= 5.0 Hz, $H_{β\text{-pyrrolic}}$), 8.82-8.76 (m, 3H, $H_{β\text{-pyrrolic}}$), 8.71 (d, 1H, ^{3}J= 5.0 Hz, $H_{β\text{-pyrrolic}}$), 8.31-8.28 (m, 2H, $H_{o\text{-Ar}}$), 8.23-8.15 (m, 6H, $H_{o\text{-Ar}}$), 7.82-7.67 (m, 12H, $H_{m,p\text{-Ar}}$), 7.45 (s, 1H, H_{vinyl}), 7.29 (d, 2H, ^{3}J=9.0, H_{AR}), 6.90 (d, 2H, ^{3}J=9.0, H_{AR}), 3.88 (s, 3H, H_{OMe}), -2.59 (br s, 2H, NH). UV-vis (CH_2Cl_2) $λ_{max}$ (log ε) 429 (4.97), 524 (3.96), 566 (3.60), 601 (3.50), 658 (3.26) nm. HRMS, *m/z*: calcd for MH^+ ($C_{54}H_{37}N_5O$): 772.3076, found: 772.3094.

9

A solution of 2-formyl-5,10,15,20-tetraphenylporphyrin **1** (30 mg, 47 µmol) and methyl 4-(cyanomethyl)benzoate **4** (49 mg, 0.28 mmol) in CH_2Cl_2 (8 mL) was stirred at room temperature under argon. Excess DBU (0.5 mL) was added and stirred for 30 min. The reaction mixture was directly purified by flash chromatography (silica, CH_2Cl_2) and concentrated *in vacuo*. Crystallisation in CH_2Cl_2/MeOH gave the desired product **9** (33 mg, 84%) as a purple solid. ^{1}H-NMR (400 MHz, $CDCl_3$): δ 9.51 (s, 1H, $H_{β\text{-pyrrolic}}$), 8.95 (d, 1H, ^{3}J= 5.0 Hz, $H_{β\text{-pyrrolic}}$), 8.88 (d, 1H, ^{3}J= 5.0 Hz, $H_{β\text{-pyrrolic}}$), 8.82 (d, 1H, ^{3}J= 5.0 Hz, $H_{β\text{-pyrrolic}}$), 8.78 (d, 1H,

^{3}J= 5.0 Hz, $H_{\beta\text{-pyrrolic}}$), 8.76 (d, 1H, ^{3}J= 5.0 Hz, $H_{\beta\text{-pyrrolic}}$), 8.72 (d, 1H, ^{3}J= 5.0 Hz, $H_{\beta\text{-pyrrolic}}$), 8.31-8.27 (m, 2H, $H_{o\text{-Ar}}$), 8.22-8.13 (m, 6H, $H_{o\text{-Ar}}$), 8.02 (d, 2H, ^{3}J= 9.0 Hz, H_{AR}), 7.82-7.63 (m, 13H, $H_{m,p\text{-Ar}}$ + H_{vinyl}), 7.38 (d, 2H, ^{3}J= 9.0 Hz, H_{AR}), 3.97 (s, 3H, CO_2CH_3), -2.57 (br s, 2H, NH). UV-vis (CH_2Cl_2) λ_{max} (log ε) 432 (5.29), 525 (4.35), 570 (3.96), 603 (3.92), 663 (3.89) nm. HRMS, *m/z*: calcd for MH^+ ($C_{55}H_{37}N_5O_2$): 800.3026, found: 800.3148.

10

In a 10-mL microwave reaction vial, a solution of 2-formyl-5,10,15,20-tetrakis(3,5-dimethylphenyl)porphyrin **2** (60 mg, 79 µmol), phenylacetonitrile **5** (93 mg, 0.79 mmol), DBU (1.5 mL) in 1,2-dichloroethane (2.1 mL). The reaction was heated at 100 ^{0}C, power 250 W for 50 min under microwave irradiation. The cooled reaction was then purified by flash chromatography (silica, 4:1 CH_2Cl_2/hexane) and crystallisation from CH_2Cl_2/MeOH, to give the desired product **10** (25 mg, 37%) as a purple-brown solid. ^{1}H-NMR (400 MHz, $CDCl_3$): δ 9.51 (s, 1H, $H_{\beta\text{-pyrrolic}}$), 9.00 (d, 1H, ^{3}J= 5.0, $H_{\beta\text{-pyrrolic}}$), 8.90 (d, 1H, ^{3}J= 5.0, $H_{\beta\text{-pyrrolic}}$), 8.85 (d, 1H, ^{3}J= 5.0, $H_{\beta\text{-pyrrolic}}$), 8.83-8.78 (m, 3H, $H_{\beta\text{-pyrrolic}}$),7.94 (s, 2H,$H_{o\text{-Xyl}}$), 7.83 (s, 2H, $H_{o\text{-Xyl}}$), 7.82 (s, 2H, $H_{o\text{-Xyl}}$), 7.80 (s, 2H, $H_{o\text{-Xyl}}$), 7.62 (s, 1H, H_{vinyl}), 7.45-7.37 (m, 8H, $H_{p\text{-Xyl}}$ + H_{AR}), 7.24 (s, 1H, $H_{p\text{-Xyl}}$), 2.65 (s, 6H, $H_{Me\text{-Xyl}}$), 2.61 (s, 6H, $H_{Me\text{-Xyl}}$), 2.60 (s, 6H, $H_{Me\text{-Xyl}}$), 2.46 (s, 6H, $H_{Me\text{-Xyl}}$), -2.61 (br s, 2H, NH). UV-vis (CH_2Cl_2) λ_{max} (log ε) 433 (5.29), 526.5 (4.21), 567 (3.85), 604 (3.79), 664 (3.83) nm. HRMS, *m/z*: calcd for MH^+ ($C_{61}H_{51}N_5$): 854.4223, found: 854.4418.

11

A solution of 2-formyl-5,10,15,20-tetrakis(3,5-dimethylphenyl)porphyrin **2** (60 mg, 79 µmol), 4-methoxyphenylacetonitrile **6** (231 mg, 1.6 mmol), KOtBu (100 mg) in DMF (2.1 mL) was heated to 100 ^{0}C for 20 min in a microwave reactor (250 W). The cooled reaction was then purified by flash chromatography (silica, CH_2Cl_2) and crystallisation from CH_2Cl_2/MeOH, to give the desired product **11** (41 mg, 59%) as a purple-brown solid. ^{1}H-NMR (400 MHz, $CDCl_3$): δ 9.48 (s, 1H, $H_{\beta\text{-pyrrolic}}$), 8.98 (d, 1H, ^{3}J= 5.0, $H_{\beta\text{-pyrrolic}}$), 8.89 (d, 1H, ^{3}J= 5.0, $H_{\beta\text{-pyrrolic}}$), 8.84 (d, 1H, ^{3}J= 5.0, $H_{\beta\text{-pyrrolic}}$), 8.82-8.78 (m, 3H, $H_{\beta\text{-pyrrolic}}$), 7.93 (s, 2H,$H_{o\text{-Xyl}}$), 7.83 (s, 2H,$H_{o\text{-Xyl}}$), 7.82 (s, 2H,$H_{o\text{-Xyl}}$), 7.80 (s, 2H,$H_{o\text{-Xyl}}$), 7.48 (s, 1H, H_{vinyl}), 7.44-7.39 (m, 3H, $H_{p\text{-Xyl}}$),7.36 (d, 2H, ^{3}J= 9.5, H_{AR}), 7.27 (s, 1H, $H_{p\text{-Xyl}}$), 6.93 (d, 2H, ^{3}J= 9.5, H_{AR}), 3.91 (S,3H, H_{OMe}), 2.64 (s, 6H, $H_{Me\text{-Xyl}}$), 2.61 (s, 6H, $H_{Me\text{-Xyl}}$), 2.60 (s, 6H, $H_{Me\text{-Xyl}}$), 2.47 (s, 6H, $H_{Me\text{-Xyl}}$), -2.61 (br s, 2H, NH). UV-vis (CH_2Cl_2) λ_{max} (log ε) 431 (5.54), 525 (4.45), 567 (4.19), 603 (4.14), 664.5 (4.15) nm. HRMS, *m/z*: calcd for MH^+ ($C_{62}H_{53}N_5O$): 884.4328, found: 884.4579.

12

A solution of 2-formyl-5,10,15,20-tetrakis(3,5-dimethylphenyl)porphyrin **2** (200 mg, 0.265 mmol) and methyl 4-(cyanomethyl)benzoate **4** (140 mg, 0.799 mmol) in CH_2Cl_2 (15 mL) was stirred at room temperature under argon. Excess DBU (1.6 mL) was added and stirred for 60 min. The reaction mixture was directly purified by flash chromatography (silica, CH_2Cl_2) and concentrated *in vacuo*. Crystallisation in CH_2Cl_2/MeOH gave the desired product **13** (224 mg, 93%) as a purple solid. ^{1}H-NMR (400 MHz, $CDCl_3$): δ 9.48 (s, 1H, $H_{\beta\text{-pyrrolic}}$), 8.93 (d, 1H, ^{3}J= 5.0 Hz, $H_{\beta\text{-pyrrolic}}$), 8.83 (d, 1H, ^{3}J= 5.0 Hz, $H_{\beta\text{-pyrrolic}}$), 8.79 (d, 1H, ^{3}J= 5.0 Hz, $H_{\beta\text{-pyrrolic}}$), 8.76-8.70 (m, 3H, $H_{\beta\text{-pyrrolic}}$),7.99 (s, 2H, H_{AR}), 7.86 (s, 2H, $H_{o\text{-Xyl}}$), 7.77-7.73 (m, 6H, $H_{o\text{-Xyl}}$), 7.66 (s, 1H, H_{vinyl}), 7.42 (d, 2H, ^{3}J= 9.0 Hz, H_{AR}), 7.36 (s, 1H, $H_{p\text{-Xyl}}$), 7.33 (s, 2H, $H_{p\text{-Xyl}}$), 7.20 (s, 1H, $H_{p\text{-Xyl}}$), 3.92 (s, 3H, CO_2CH_3), 2.57 (s, 6H, $H_{Me\text{-Xyl}}$), 2.53 (s, 6H, $H_{Me\text{-Xyl}}$), 2.52 (s, 6H, $H_{Me\text{-Xyl}}$), 2.40 (s, 6H, $H_{Me\text{-Xyl}}$), -2.66 (br s, 2H, NH). UV-vis (CH_2Cl_2) λ_{max} (log ε) 436 (4.97), 527 (4.01), 569 (3.63), 604 (3.59), 663 (3.42) nm. HRMS, *m/z*: calcd for MH^+ ($C_{63}H_{53}N_5O_2$): 912.4278, found: 912.4244.

13

A solution of 2-formyl-5,10,15,20-tetrakis(3,5-dimethylphenyl)porphyrin **2** (76 mg, 0.100 mmol) and methyl 4-(cyanomethyl)benzonitrile **3** (46 mg, 0.300 mmol) in CH_2Cl_2 (15 mL) was stirred at room temperature under argon. Excess DBU (1.6 mL) was added and stirred for 60 min. The reaction mixture was directly purified by flash chromatography (silica, CH_2Cl_2) and concentrated *in vacuo*. Crystallisation in CH_2Cl_2/MeOH gave the desired product **13** (70 mg, 80%) as a purple solid. ^{1}H-NMR (400 MHz, $CDCl_3$): δ 9.55 (d, 1H, ^{3}J= 1.0 Hz, $H_{\beta\text{-pyrrolic}}$), 9.01 (d, 1H, ^{3}J= 4.7 Hz, $H_{\beta\text{-pyrrolic}}$), 8.90 (d, 1H, ^{3}J= 4.7 Hz, $H_{\beta\text{-pyrrolic}}$), 8.86 (d, 1H, ^{3}J= 4.7 Hz, $H_{\beta\text{-pyrrolic}}$), 8.82 (d, 1H, ^{3}J= 4.7 Hz, $H_{\beta\text{-pyrrolic}}$), 8.80 (d, 1H, ^{3}J= 4.7 Hz, $H_{\beta\text{-pyrrolic}}$), 8.78 (d, 1H, ^{3}J= 4.7 Hz, $H_{\beta\text{-pyrrolic}}$), 8.10-8.05 (m, 2H, H_{AR}), 7.95-7.92 (m, 2H, $H_{o\text{-Xyl}}$), 7.85-7.80 (m, 6H, $H_{o\text{-Xyl}}$), 7.74 (d, 1H, ^{3}J= 1.0 Hz, H_{vinyl}), 7.53-7.48 (m, 2H, H_{AR}), 7.45-7.39 (m, 3H, $H_{p\text{-Xyl}}$), 7.28-7.27 (m, 1H, $H_{p\text{-Xyl}}$), 2.65 (s, 6H, $H_{Me\text{-Xyl}}$), 2.61 (s, 6H, $H_{Me\text{-Xyl}}$), 2.60 (s, 6H, $H_{Me\text{-Xyl}}$), 2.47 (s, 6H, $H_{Me\text{-Xyl}}$), -2.59 (br s, 2H, NH). UV-vis (CH_2Cl_2) λ_{max} (log ε) 432 (5.47), 527 (4.54), 570 (4.15), 603 (4.11), 662 (3.99) nm. HRMS, *m/z*: calcd for M^+ ($C_{62}H_{50}N_6$): 878.4097, found: 878.4057.

General Zinc Insertion Procedure

Porphyrin monomers were converted to zinc (II) porphyrins according to the following general procedure. Cyano-linked porphyrin was dissolved in CH_2Cl_2 and stirred at room temperature. 1.3 equivilants of $Zn(OAc)_2{\cdot}2H_2O$ in minimal amount of methanol were added and continued to stir for 30 min. MALDI indicated the reaction was complete and flash chromatography (silica, CH_2Cl_2) and concentration *in vacuo* gave the desired products.

Zn7

Porphyrin **7** (12 mg, 17 µmol) was reacted with $Zn(OAc)_2{\cdot}2H_2O$. **Zn7** was collected as a purple solid (10 mg, 71%). ^{1}H-NMR (400 MHz, $CDCl_3$): δ 9.59 (s, 1H, $H_{\beta\text{-pyrrolic}}$), 9.00 (d, 1H, ^{3}J= 5.0 Hz, $H_{\beta\text{-pyrrolic}}$), 8.95-8.91 (m, 3H, $H_{\beta\text{-pyrrolic}}$), 8.88 (d, 1H, ^{3}J= 5.0 Hz, $H_{\beta\text{-pyrrolic}}$), 8.76 (d, 1H, ^{3}J= 5.0 Hz, $H_{\beta\text{-pyrrolic}}$), 8.29-8.13 (m, 8H, $H_{o\text{-Ar}}$), 7.81-7.64 (m, 13H, $H_{m,p\text{-Ar}}$ + H_{vinyl}), 7.39-7.34 (m, 5H, H_{AR}). UV-vis (CH_2Cl_2) λ_{max} (log ε) 433 (5.47), 558 (4.41), 598 (4.14) nm. HRMS, *m/z*: calcd for MH^+ ($C_{53}H_{33}N_5Zn$): 804.2106, found: 804.5568.

Zn8

Porphyrin **8** (32 mg, 41 µmol) was reacted with $Zn(OAc)_2{\cdot}2H_2O$. **Zn8** was collected as a purple solid (28 mg, 82%). ^{1}H-NMR (400 MHz, $CDCl_3$): δ9.50 (s, 1H, $H_{\beta\text{-pyrrolic}}$), 8.99 (d, 1H, ^{3}J= 5.0 Hz, $H_{\beta\text{-pyrrolic}}$), 8.95-8.86 (m, 4H, $H_{\beta\text{-pyrrolic}}$), 8.75 (d, 1H, ^{3}J= 5.0 Hz, $H_{\beta\text{-pyrrolic}}$), 8.26-8.17 (m, 6H, $H_{o\text{-Ar}}$), 8.15-8.10 (m, 2H, $H_{o\text{-Ar}}$), 7.80-7.71 (m, 10H, $H_{m,p\text{-Ar}}$), 7.68-7.63 (m, 2H $H_{m\text{-Ar}}$) 7.47 (s, 1H, H_{vinyl}), 7.22 (d, 2H, ^{3}J=9.0, H_{AR}), 6.83 (d, 2H, ^{3}J=9.0, H_{AR}), 3.82 (s, 3H, H_{OMe}). UV-vis (CH_2Cl_2) λ_{max} (log ε) 432 (5.59), 558 (4.56), 598 (4.28) nm. HRMS, m/z: calcd for MH+ ($C_{62}H_{52}N_5OZn$): 946.3463, found: 946.3771.

Zn9

Porphyrin **9** (40 mg, 44 µmol) was reacted with $Zn(OAc)_2{\cdot}2H_2O$. **Zn9** was collected as a purple solid (28 mg, 93%). ^{1}H-NMR (400 MHz, $CDCl_3$): δ 9.62 (d, 1H, ^{4}J= 1.0 Hz, $H_{\beta\text{-pyrrolic}}$), 9.00 (d, 1H, ^{3}J= 5.0 Hz, $H_{\beta\text{-pyrrolic}}$), 8.95-8.87 (m, 4H, $H_{\beta\text{-pyrrolic}}$), 8.75 (d, 1H, ^{3}J= 5.0 Hz, $H_{\beta\text{-pyrrolic}}$), 8.29-8.14 (m, 8H, $H_{o\text{-Ar}}$), 7.98 (d, 2H, ^{3}J= 9.0 Hz, H_{AR}), 7.81-7.65 (m, 13H, $H_{m,p\text{-Ar}}$ + H_{vinyl}), 7.39 (d, 2H, ^{3}J= 9.0 Hz, H_{AR}), 3.92 (s, 3H, CO_2CH_3). UV-vis (CH_2Cl_2) λ_{max} (log ε) 439 (4.65), 559 (3.68), 603 (3.51) nm. HRMS, m/z: calcd for M+ ($C_{55}H_{35}N_5O_2Zn$): 861.2082, found: 861.2116.

Zn10

Porphyrin **10** (42 mg, 49 µmol) was reacted with $Zn(OAc)_2{\cdot}2H_2O$. **Zn10** was collected as a purple solid (40 mg, 89%). ^{1}H-NMR (400 MHz, $CDCl_3$): δ 9.65 (s, 1H, $H_{\beta\text{-pyrrolic}}$), 9.07 (d, 1H, ^{3}J=4.5 Hz, $H_{\beta\text{-pyrrolic}}$), 8.97 (d, 1H, ^{3}J=4.5 Hz, $H_{\beta\text{-pyrrolic}}$), 8.95-8.91 (m, 3H, $H_{\beta\text{-pyrrolic}}$), 8.87 (d, 1H, ^{3}J=4.5 Hz, $H_{\beta\text{-pyrrolic}}$), 7.94 (s, 2H, $H_{o\text{-Xyl}}$), 7.84 (s, 2H, $H_{o\text{-Xyl}}$), 7.83 (s, 2H, $H_{o\text{-Xyl}}$), 7.79 (s, 2H, $H_{o\text{-Xyl}}$), 7.70 (s, 1H, H_{vinyl}) 7.46-7.36 (m, 8H, $H_{p\text{-Xyl}}$ + H_{AR}), 7.23 (S, 1H, $H_{p\text{-Xyl}}$), 2.64 (s, 6H, $H_{Me\text{-Xyl}}$), 2.60 (s, 6H, $H_{Me\text{-Xyl}}$), 2.59 (s, 6H, $H_{Me\text{-Xyl}}$), 2.44 (s, 6H, $H_{Me\text{-Xyl}}$). UV-vis (CH_2Cl_2) λ_{max} (log ε) 437.5 (5.45), 559 (4.40), 600.5 (4.12) nm. HRMS, *m/z*: calcd for MH^+ ($C_{61}H_{49}N_5Zn$): 916.3358, found: 916.3765.

Zn11

Porphyrin **11** (42 mg, 48 µmol) was reacted with $Zn(OAc)_2{\cdot}2H_2O$. **Zn11** was collected as a purple solid (44 mg, 98%). ^{1}H-NMR (400 MHz, $CDCl_3$): δ 9.54 (s, 1H, $H_{\beta\text{-pyrrolic}}$), 8.99 (d, 1H, ^{3}J= 4.5, $H_{\beta\text{-pyrrolic}}$), 8.90 (d, 1H, ^{3}J= 4.5, $H_{\beta\text{-pyrrolic}}$), 8.87-8.83 (m, 3H, $H_{\beta\text{-pyrrolic}}$), 8.79 (d, 1H, ^{3}J= 4.5, $H_{\beta\text{-pyrrolic}}$), 7.79 (s, 2H,$H_{o\text{-Xyl}}$), 7.76 (s, 2H,$H_{o\text{-Xyl}}$), 7.75 (s, 2H,$H_{o\text{-Xyl}}$), 7.70 (s, 2H,$H_{o\text{-Xyl}}$), 7.48 (s, 1H, H_{vinyl}), 7.36-7.32 (m, 3H, $H_{p\text{-Xyl}}$), 7.30 (d, 2H, ^{3}J= 9.0, H_{AR}), 7.18 (s, 1H, $H_{p\text{-Xyl}}$), 6.82 (d, 2H, ^{3}J= 9.5, H_{AR}), 3.78 (S,3H, H_{OMe}), 2.57 (s, 6H, $H_{Me\text{-Xyl}}$), 2.53 (s, 6H, $H_{Me\text{-Xyl}}$), 2.52 (s, 6H, $H_{Me\text{-Xyl}}$), 2.38 (s, 6H, $H_{Me\text{-Xyl}}$). UV-vis (CH_2Cl_2) λ_{max} (log ε) 436 (2.336), 559 (4.55), 599.5 (4.27) nm. HRMS, *m/z*: calcd for MH^+ ($C_{62}H_{51}N_5OZn$): 946.3463, found: 946.3771.

Zn12

Porphyrin **12** (40 mg, 44 µmol) was reacted with $Zn(OAc)_2{\cdot}2H_2O$. **Zn12** was collected as a purple solid (40 mg, 93%). ^{1}H-NMR (400 MHz, $CDCl_3$): δ 9.63 (d, 1H, ^{4}J= 1.0 Hz, $H_{\beta\text{-pyrrolic}}$), 8.99 (d, 1H, ^{3}J= 5.0 Hz, $H_{\beta\text{-pyrrolic}}$), 8.89 (d, 1H, ^{3}J= 5.0 Hz, $H_{\beta\text{-pyrrolic}}$), 8.87-8.34 (m, 3H, $H_{\beta\text{-pyrrolic}}$), 8.79 (d, 1H, ^{3}J= 5.0 Hz, $H_{\beta\text{-pyrrolic}}$), 7.99 (d, 2H, ^{3}J= 9.0 Hz, H_{AR}), 7.86 (s, 2H, $H_{o\text{-Xyl}}$), 7.78-7.71 (m, 7H, $H_{o\text{-Xyl}}$ and H_{vinyl}), 7.45 (d, 2H, ^{3}J= 9.0 Hz, H_{AR}), 7.36 (s, 1H, $H_{p\text{-Xyl}}$), 7.33 (s, 2H, $H_{p\text{-Xyl}}$), 7.20 (s, 1H, $H_{p\text{-Xyl}}$), 3.91 (s, 3H, CO_2CH_3), 2.57 (s, 6H, $H_{Me\text{-Xyl}}$), 2.53 (s, 6H, $H_{Me\text{-Xyl}}$), 2.52 (s, 6H, $H_{Me\text{-Xyl}}$), 2.39 (s, 6H, $H_{Me\text{-Xyl}}$). UV-vis (CH_2Cl_2) λ_{max} (log ε) 444 (5.11), 561 (4.12), 604 (3.98) nm. HRMS, *m/z*: calcd for MH^+ ($C_{63}H_{51}N_5O_2Zn$): 974.3412, found: 974.3650.

Zn13

Porphyrin **13** (40 mg, 44 µmol) was reacted with $Zn(OAc)_2{\cdot}2H_2O$. **Zn13** was collected as a purple solid (73 mg, 93%). ^{1}H-NMR (400 MHz, $CDCl_3$): δ 9.20 (d, 1H, ^{3}J= 1.1 Hz, $H_{\beta\text{-pyrrolic}}$), 9.06 (d, 1H, ^{3}J= 4.7 Hz, $H_{\beta\text{-pyrrolic}}$), 8.97 (d, 1H, ^{3}J= 4.7 Hz, $H_{\beta\text{-pyrrolic}}$), 8.94-8.93 (m, 2H, $H_{\beta\text{-pyrrolic}}$), 8.92 (d, 1H, ^{3}J= 4.7 Hz, $H_{\beta\text{-pyrrolic}}$), 8.86 (d, 1H, ^{3}J= 4.7 Hz, $H_{\beta\text{-pyrrolic}}$),8.09-8.06 (m, 2H, H_{AR}), 7.94-7.92 (m, 2H, $H_{o\text{-Xyl}}$), 7.84 (d, 1H, ^{3}J= 1.0 Hz, $H_{o\text{-Xyl}}$), 7.83-7.79 (m, 6H, $H_{o\text{-Xyl}}$), 7.55-7.51 (m, 2H, H_{AR}), 7.44-7.39 (m, 3H, $H_{p\text{-Xyl}}$), 7.23-7.26 (m, 1H, $H_{p\text{-Xyl}}$), 2.66 (s, 6H, $H_{Me\text{-Xyl}}$), 2.61 (s, 6H, $H_{Me\text{-Xyl}}$), 2.60 (s, 6H, $H_{Me\text{-Xyl}}$), 2.46 (s, 6H, $H_{Me\text{-Xyl}}$). UV-vis (CH_2Cl_2) λ_{max} (log ε) 445 (5.16), 562 (4.18), 606 (4.03) nm.

Zn25

KOH (46 mg, 0.71 mmol) in MeOH (12 mL)/H_2O (1.2 mL) was added to a solution of **Zn12** (40 mg, 0.041 mmol) in THF (12 mL). The mixture was heated to reflux for 22 h. Once cooled to room temperature, H_2O (25 mL) and CH_2Cl_2 (25 mL) were added followed by 2M H_3PO_4 (430 µL, 0.86 mmol). The organic layer was extracted and washed with H_2O (2 x 40 mL). Reaction was concentrated *in vacuo* to give the desired product **Zn25** (39 mg, 100%) as a purple solid. ^{1}H-NMR (400 MHz, acetone-d_6): δ 9.64(s, 1H, $H_{\beta\text{-pyrrolic}}$), 8.97 (d, 1H, ^{3}J= 5.0 Hz, $H_{\beta\text{-pyrrolic}}$), 8.88 (d, 1H, ^{3}J= 5.0 Hz, $H_{\beta\text{-pyrrolic}}$), 8.86-8.81 (m, 4H, $H_{\beta\text{-pyrrolic}}$), 8.16 (d, 2H, ^{3}J= 8.0 Hz, H_{AR}), 7.96 (s, 1H, H_{vinyl}), 7.92 (s, 2H, $H_{o\text{-Xyl}}$), 7.86-7.80 (m, 6H, $H_{o\text{-Xyl}}$), 7.62 (d, 2H, ^{3}J= 8.0 Hz, H_{AR}), 7.49-7.44 (m, 3H, $H_{p\text{-Xyl}}$), 7.37 (s, 1H, $H_{p\text{-Xyl}}$), 2.64 (s, 6H, $H_{Me\text{-Xyl}}$), 2.61 (s, 6H, $H_{Me\text{-Xyl}}$), 2.61 (s, 6H, $H_{Me\text{-Xyl}}$), 2.50 (s, 6H, $H_{Me\text{-Xyl}}$). UV-vis (DMF) λ_{max} (log ε) 445 (5.05), 571 (4.05), 616 (3.88) nm. HRMS, *m/z*: calcd for MH^+ ($C_{62}H_{49}N_5O_2Zn$): 960.3256, found: 960.3373.

Synthesis of Porphyrin Dyads
General Procedure

A solution of 2-formyl porphyrin (60 mg), 1,4-phenylenediacetonitrile **15** (10 equivalents), 1,8-diazabicycoundec-7-ene (DBU) (1.5 mL) and dichloroethane (2.1 mL) was heated for 30 min at 100 ^{0}C and 250 W in a microwave reactor. The cooled reaction was then purified by column chromatography (silica, CH_2Cl_2) and crystalised in CH_2Cl_2/MeOH to give the desired compounds.

16

A solution of 2-formyl-5,10,15,20-tetrakis(4-methylphenyl)porphyrin **14** (60 mg, 86 µmol) 1,4-phenylenediacetonitrile **15** (7 mg, 43 µmol) in $CHCl_3$ (3 mL) was stirred at room temperature under argon. Excess DBU (0.5 mL) was added and stirred for 4 hrs. The reaction mixture was directly purified by flash chromatography (silica, CH_2Cl_2:Hexane (7:3)) and concentrated *in vacuo*. Crystallisation in CH_2Cl_2/MeOH gave the desired product **16** (8 mg, 12%) as a purple solid. ^{1}H-NMR (400 MHz, $CDCl_3$): δ 9.56 (s, 2H, $H_{\beta\text{-pyrrolic}}$), 8.97 (d, 2H, ^{3}J= 5.0 Hz, $H_{\beta\text{-pyrrolic}}$), 8.90 (d, 2H, ^{3}J= 5.0 Hz, $H_{\beta\text{-pyrrolic}}$), 8.87 (d, 2H, ^{3}J= 5.0 Hz, $H_{\beta\text{-pyrrolic}}$), 8.84-8.78 (m, 6H, $H_{\beta\text{-pyrrolic}}$), 8.23 (d, 4H, ^{3}J= 8.0 Hz, $H_{o\text{-Tol}}$), 8.15-8.07 (m, 12H, $H_{o\text{-Tol}}$), 7.68-7.64 (m, 6H, $H_{m\text{-Tol}}$ and H_{vinyl}), 7.60-7.55 (m, 12H, $H_{m\text{-Tol}}$), 7.46 (s, 2H, H_{AR}), 2.75 (s, 6H, $H_{Me\text{-Tol}}$), 2.71 (s, 12H, $H_{Me\text{-Tol}}$), 2.60 (s, 6H, $H_{Me\text{-Tol}}$), -2.55 (br s, 4H, NH). UV-vis (CH_2Cl_2) λ_{max} (log ε) 431 (5.49), 527 (4.68), 573.5 (4.31), 601 (4.25), 662 (4.02) nm. HRMS, *m/z*: calcd for MH^+ ($C_{108}H_{80}N_{80}$): 1517.6646, found: 1517.7460.

18

18 was collected as a purple solid (58 mg, 80%). ^{1}H-NMR (400 MHz, $CDCl_3$): δ 9.50 (s, 1H, $H_{\beta\text{-pyrrolic}}$), 8.95 (d, 1H, ^{3}J= 5.0 Hz, $H_{\beta\text{-pyrrolic}}$), 8.88 (d, 1H, ^{3}J= 5.0 Hz, $H_{\beta\text{-pyrrolic}}$), 8.83 (d, 1H, ^{3}J= 5.0 Hz, $H_{\beta\text{-pyrrolic}}$), 8.79 (d, 1H, ^{3}J= 5.0 Hz, $H_{\beta\text{-pyrrolic}}$), 8.77 (d, 1H, ^{3}J= 5.0 Hz, $H_{\beta\text{-pyrrolic}}$), 8.73 (d, 1H, ^{3}J= 5.0 Hz, $H_{\beta\text{-pyrrolic}}$), 8.32-8.28 (m, 2H, $H_{o\text{-Ph}}$), 8.23-8.18 (m, 6H, $H_{o\text{-Ph}}$), 7.84-7.70 (m, 12H, $H_{m,p\text{-Ph}}$) 7.63 (s, 1H, H_{vinyl}), 7.38-7.34 (m, 4H, H_{AR}), 3.82 (s, 2H, $H_{Benzylic}$), -2.58 (br s, 2H, NH). UV-vis (CH_2Cl_2) λ_{max} (log ε) 431 (5.22), 525 (420),

567 (3.82), 602 (3.76), 660 (3.57) nm. HRMS, *m/z*: calcd for MH^+ ($C_{55}H_{36}N_6$): 781.3080, found: 781.3079.

Fe18

10 mL of acetonitrile was refluxed under argon for 2 hrs to remove any dissolved oxygen. The reaction's temperature was then lowered to 70 ^oC and iron (II) chloride (190mg, 0.96 mmol) added. A solution of **18** (34mg, 0.044 mmol) in 5 mL of degased chloroform was then added to the reaction over 5 mi. The reaction was then heated back up to reflux, stirred for 3 hrs and then left exposed to air overnight at room temperature. The reaction was then concentrated *in vacuo*, redissolved in dichloromethane and washed with 0.1M HCl (3 x 25 mL). The reaction was purified by column chromatography (silica, 100% dichloromethane - 98% dichloromethane: 2% methanol) and filtered through filter paper to give the desired compound **Fe18** as a purple/brown solid (22 mg, 58%). UV-vis (CH_2Cl_2) λ_{max} (log ε) 433 (4.94), 515 (4.06), 668 (3.36) nm. HRMS, *m/z*: calcd for MH^+-Cl^- ($C_{55}H_{34}FeN_6$): 834.2194, found: 834.2316.

19

19 was collected as a purple solid (55 mg, 78%). ^{1}H-NMR (400 MHz, $CDCl_3$): δ 9.53 (s, 1H, $H_{β\text{-}pyrrolic}$), 9.00 (d, 1H, ^{3}J= 5.0 Hz, $H_{β\text{-}pyrrolic}$), 8.90 (d, 1H, ^{3}J= 5.0 Hz, $H_{β\text{-}pyrrolic}$), 8.86 (d, 1H, ^{3}J= 5.0 Hz, $H_{β\text{-}pyrrolic}$), 8.82-8.77 (m, 3H, $H_{β\text{-}pyrrolic}$), 7.94 (s, 2H, $H_{o\text{-}Xyl}$), 7.84-7.80 (m, 6H, $H_{o\text{-}Xyl}$), 7.65 (s, 1H, H_{Vinyl}), 7.46-7.35 (m, 7H, $H_{p\text{-}Xyl}$ + H_{AR}), 7.23 (s, 1H, $H_{p\text{-}Xyl}$), 3.84 (s, 2H, $H_{Benzylic}$), 2.65 (s, 6H, $H_{Me\text{-}Xyl}$), 2.61 (s, 6H, $H_{Me\text{-}Xyl}$), 2.60 (s, 6H, $H_{Me\text{-}Xyl}$), 2.48 (s, 6H, $H_{Me\text{-}Xyl}$), -2.60 (br s, 2H, NH). UV-vis (CH_2Cl_2) λ_{max} (log ε) 435 (5.49), 527 (4.48), 568 (4.07), 604 (4.01) 662 (3.94) nm. HRMS, *m/z*: calcd for MH^+ ($C_{63}H_{52}N_6$): 893.4332, found: 893.4468.

20

20 was collected as a purple solid (48 mg, 68%). ^{1}H-NMR (400 MHz, $CDCl_3$): δ 9.45 (s, 1H, $H_{β\text{-}pyrrolic}$), 8.96 (d, 1H, ^{3}J= 5.0 Hz, $H_{β\text{-}pyrrolic}$), 8.89 (d, 1H, ^{3}J= 5.0 Hz, $H_{β\text{-}pyrrolic}$), 8.84 (d, 1H, ^{3}J= 5.0 Hz, $H_{β\text{-}pyrrolic}$), 8.81-8.74 (m, 3H, $H_{β\text{-}pyrrolic}$), 8.21 (d, 2H, ^{3}J=7.5, $H_{o\text{-}Ar}$), 8.12 (d, 2H, ^{3}J=7.5, $H_{o\text{-}Ar}$), 8.10 (d, 2H, ^{3}J=7.5, $H_{o\text{-}Ar}$), 8.04 (d, 2H, ^{3}J=7.5, $H_{o\text{-}Ar}$), 7.63 (d, 2H, ^{3}J=7.5, $H_{m\text{-}Ar}$), 7.60-7.54 (m, 4H, $H_{m\text{-}Ar}$), 7.52 (s, 1H, H_{Vinyl}), 7.46 (d, 2H, ^{3}J=7.5, $H_{m\text{-}Ar}$), 7.37 (d, 2H, ^{3}J=8.0, H_{AR}), 7.30 (d, 2H, ^{3}J=8.0, H_{AR}), 3.77 (s, 2H, $H_{Benzylic}$), 3.04-2.96 (m, 6H, C**H**$_2$CH$_3$), 2.78 (q, 2H, ^{3}J=7.5, C**H**$_2$CH$_3$), 1.55-1.50 (m, 9H, CH$_2$C**H**$_3$), 1.29 (t, 3H, ^{3}J=7.5, CH$_2$C**H**$_3$), -2.58 (br s, 2H, NH). UV-vis (CH_2Cl_2) λ_{max} (log ε) 433 (4.66) 527 (3.68) 565 (3.37) 603 (3.29) 660 (3.16) nm. HRMS, *m/z*: calcd for MH^+ ($C_{63}H_{52}N_6$): 893.4332, found: 893.4310.

21

A solution of 2-formyl-5,10,15,20-tetrakis(3,5-dimethylphenyl)porphyrin **2** (12 mg, 15 µmol), cyano porphyrin **20** (5.5 mg, 6.2 µmol) and DBU (0.2 mL) in DCE (0.2 mL) was heated to 120 ^{0}C, 250 W for 30 min in a microwave reactor. The cooled reaction was then purified by flash chromatography (silica, CH_2Cl_2:Hexane (4:1)) and crystallisation from CH_2Cl_2/MeOH, to give the desired product **16** (8 mg, 80%) as a purple/brown solid. ^{1}H-NMR (400 MHz, $CDCl_3$): δ 9.60 (s, 1H, $H_{β\text{-}pyrrolic}$), 9.55 (s, 1H, $H_{β\text{-}pyrrolic}$), 9.03-8.97 (m, 2H, $H_{β\text{-}pyrrolic}$), 8.93-8.78 (m, 10H, $H_{β\text{-}pyrrolic}$), 8.28-8.24 (m, 2H, $H_{o\text{-}Ar}$), 8.17-8.11 (m, 6H, $H_{o\text{-}Ar}$), 7.98 (s, 2H, $H_{o\text{-}Xyl}$), 7.87-7.82 (m, 6H, $H_{o\text{-}Xyl}$), 7.72-7.66 (m, 4H, $H_{m\text{-}Ar}$ and H_{vinyl}), 7.63-7.55 (m, 6H, $H_{m\text{-}Ar}$), 7.53-7.34 (m, 8H, $H_{p\text{-}Xyl}$ and H_{AR}), 3.02 (m, 6H, C**H**$_2$CH$_3$), 2.86 (q, 2H, ^{3}J= 7.5 Hz, C**H**$_2$CH$_3$), 2.69 (s, 6H, $H_{Me\text{-}Xyl}$), 2.62 (s, 6H, $H_{Me\text{-}Xyl}$), 2.61 (s, 6H, $H_{Me\text{-}Xyl}$), 2.54 (s, 6H, $H_{Me\text{-}Xyl}$), 1.56 (m, 9H, CH$_2$C**H**$_3$), 1.36 (m, 3H, CH$_2$C**H**$_3$), -2.53 (br s, 2H, NH), -2.57 (br s, 2H, NH). UV-vis (CH_2Cl_2) λ_{max} (log ε) 435 (4.96), 527 (4.00), 563 (3.99), 606 (3.92), 662 (3.33) nm. HRMS, *m/z*: calcd for MH^+ ($C_{116}H_{96}N_{10}$): 1629.7898, found: 1629.7880.

Zn21

Porphyrin dyad **21** (4 mg, 2.5 µmol) was dissolved in CH_2Cl_2 (4 mL) and stirred at room temperature. A solution of $Zn(OAc)_2{\cdot}2H_2O$ (1.4 mg, 6.3 µmol) in MeOH (0.4 mL) was added and stirred for 30 min. MALDI indicated reaction completion and the reaction was concentrated *in vacuo*. Crystallisation in CH_2Cl_2/MeOH gave the desired product **Zn21** (4 mg, 100%) as a purple solid. ^{1}H-NMR (400 MHz, $CDCl_3$): δ 9.74 (s, 1H, $H_{β\text{-}pyrrolic}$), 9.69 (s, 1H, $H_{β\text{-}pyrrolic}$), 9.08 (d, 1H, ^{3}J= 5.0 Hz, $H_{β\text{-}pyrrolic}$), 9.05 (d, 1H, ^{3}J= 5.0 Hz, $H_{β\text{-}pyrrolic}$), 9.00-8.83 (m, 10H, $H_{β\text{-}pyrrolic}$), 8.28-8.23 (m, 2H, $H_{o\text{-}Ar}$), 8.16-8.10 (m, 6H, $H_{o\text{-}Ar}$), 7.98 (s, 2H, $H_{o\text{-}Xyl}$), 7.85-7.78 (m, 6H, $H_{o\text{-}Xyl}$), 7.70-7.66 (m, 2H, $H_{m\text{-}Ar}$), 7.62-7.54 (m, 8H, $H_{m\text{-}Ar}$ and H_{vinyl}), 7.52-7.35 (m, 8H, $H_{p\text{-}Xyl}$ and H_{AR}), 3.03 (m, 6H, C**H**$_2$CH$_3$), 2.88 (q, 2H, ^{3}J= 7.5, C**H**$_2$CH$_3$), 2.69 (s, 6H, $H_{Me\text{-}Xyl}$), 2.62 (s, 6H, $H_{Me\text{-}Xyl}$), 2.61 (s, 6H, $H_{Me\text{-}Xyl}$), 2.53 (s, 6H, $H_{Me\text{-}Xyl}$), 1.56 (m, 9H, CH$_2$C**H**$_3$), 1.38 (m, 3H, CH$_2$C**H**$_3$). UV-vis (CH_2Cl_2) λ_{max} (log ε) 420 (4.89), 559 (3.78), 606 (3.92) nm. HRMS, m/z: calcd for M+ ($C_{116}H_{92}N_{10}Zn_2$): 1752.6089, found: 1752.6138.

22

A solution of 2-formyl-5,10,15,20-tetrakis(3,5-dimethylphenyl)porphyrinato zinc **Zn2** (13 mg, 16 µmol), cyano porphyrin **20** (5.5 mg, 6.2 µmol) and sodium methoxide (10 mg) in THF (0.3mL) was heated to 120 ^{0}C, 250 W for 60 min in a microwave reactor. The cooled reaction was then purified by flash chromatography (silica, CH_2Cl_2:Hexane (9:1)) and crystallisation from CH_2Cl_2/MeOH, to give the desired product **17** (7 mg, 70%) as a purple/brown solid. ^{1}H-NMR (400 MHz, $CDCl_3$): δ 9.71 (s, 1H, $H_{β\text{-}pyrrolic}$), 9.55 (s, 1H, $H_{β\text{-}pyrrolic}$), 9.06 (d, 1H, ^{3}J= 5.0 Hz, $H_{β\text{-}pyrrolic}$), 9.01-8.78 (m, 11H, $H_{β\text{-}pyrrolic}$), 8.28 (d, 2H, ^{3}J= 9.0 Hz, $H_{o\text{-}Ar}$), 8.18-8.09 (m, 6H, $H_{o\text{-}Ar}$), 7.96 (s, 2H, $H_{o\text{-}Xyl}$), 7.85-7.81 (m, 6H, $H_{o\text{-}Xyl}$), 7.80 (s, 1H, H_{vinyl}), 7.72-7.67 (m, 3H, $H_{m\text{-}Ar}$ and H_{vinyl}), 7.63-7.55 (m, 6H, $H_{m\text{-}Ar}$), 7.48-7.34 (m, 8H, $H_{p\text{-}Xyl}$), 6.91 (d, 2H, ^{3}J= 7.0 Hz, H_{AR}), 6.58 (m, 2H, H_{AR}), 3.04 (m, 6H, C**H**$_2$CH$_3$), 2.85 (q, 2H, ^{3}J= 7.5 Hz, C**H**$_2$CH$_3$), 2.68 (s, 6H, $H_{Me\text{-}Xyl}$), 2.61 (s, 6H, $H_{Me\text{-}Xyl}$), 2.60 (s, 6H, $H_{Me\text{-}Xyl}$), 2.52 (s, 6H, $H_{Me\text{-}Xyl}$), 1.57 (m, 9H, CH$_2$C**H**$_3$), 1.29 (m, 3H, CH$_2$C**H**$_3$), -2.53 (br s, 2H, NH). UV-vis (CH_2Cl_2) λ_{max} (log ε) 435 (5.25), 562 (4.37), 606 (4.28) nm. HRMS, *m/z*: calcd for MH^+ ($C_{116}H_{94}N_{10}Zn$): 1691.7033, found: 1691.8030.

23

A solution of 2-formyl-5,10,15,20-tetrakis(3,5-dimethylphenyl)porphyrin **2** (13 mg, 40 µmol), cyano porphyrin **Fe18** (6 mg, 6.9 µmol), DBU (0.2 mL) in DCE (0.4 mL) was heated to 120 ^{0}C, 250 W for 20 min in a microwave reactor. The cooled reaction was then purified by flash chromatography (silica, CH_2Cl_2:MeOH (1:0 to 97:3)) and crystallisation from CH_2Cl_2/MeOH, to give the desired product **23** (5 mg, 45%) as a brown/purple solid. UV-vis (CH_2Cl_2) λ_{max} (log ε) 425 (5.49), 520 (4.67), 595 (4.35), 657 (4.08) nm. HRMS, *m/z*: calcd for MH^+ ($C_{108}H_{78}ClFeN_{10}$): 1606.5527, found: 1606.6536.

Zn23

Porphyrin dyad **23** (5 mg, 3.1 µmol) was dissolved in CH_2Cl_2 (4 mL) and stirred at room temperature. A solution of $Zn(OAc)_2{\cdot}2H_2O$

(1.4 mg, 4.3 µmol) in MeOH (0.4 mL) was added and stirred for 30 min. MALDI indicated reaction completion and the reaction was concentrated *in vacuo*. Crystallisation in CH_2Cl_2/MeOH gave the desired product **Zn23** (5 mg, 100%) as a purple solid. UV-vis (CH_2Cl_2) λ_{max} (log ε) 433 (5.06), 526 (4.05), 566 (3.65), 603 (3.58), 662 (3.52) nm. HRMS, m/z: calcd for M+ ($C_{108}H_{76}ClFeN_{10}Zn$): 1667.4584, found: 1667.4596.

Supporting Information (see footnote on the first page of this article): UV-visible spectra, Raman spectra and DFT calculation data, electrochemical impedance data, dye uptake and ^{1}H-NMR spectra.

Acknowledgements

Funding from an Australian Research Council (ARC) Discovery Project grant (DP120102225), the ARC Centre of Excellence Scheme (CE140100012) and support from the Materials Node of the Australian National Fabrication Facility is gratefully acknowledged.

Keywords: porphyrin • porphyrin dyad • Knoevenagel condensation • light harvesting • dye sensitised solar cell

[1] a) M. K. Panda, K. Ladomenou, A. G. Coutsolelos, *Coord. Chem. Rev.* **2012**, *256*, 2601-2627; b) L.-L. Li, E. W. Diau, *Chem. Soc. Rev.* **2013**, *42*, 291-304.

[2] a) L. Arnold, K. Müllen, *J. Porphyrins Phthalocyanines* **2011**, *15*, 757-779; b) J. Mack, N. Kobayashi, Z. Shen, in *Handbook of Porphyrin Science, Vol. 23* (Eds.: K. M. Kadish, K. M. Smith, R. Guilard), World Scientific Publishing Company, **2012**, pp. 281-371.

[3] a) N. K. Davis, M. Pawlicki, H. L. Anderson, *Org. Lett.* **2008**, *10*, 3945-3947; b) P. J. Walsh, K. C. Gordon, P. Wagner, D. L. Officer, *ChemPhysChem* **2006**, *7*, 2358-2365.

[4] a) C. Chen, H. Yeh, X. Zhang, J. Yu, *Org. Lett.* **1999**, *1*, 1767-1770; b) P. J. Walsh, K. C. Gordon, D. L. Officer, W. M. Campbell, *THEOCHEM* **2006**, *759*, 17-24.

[5] a) M. Ishida, S. Park, D. Hwang, Y. Koo, J. L. Sessler, D. Kim, D. Kim, *J. Phys. Chem. C* **2011**, *115*, 19343-19354; b) Q. Wang, W. M. Campbell, E. E. Bonfantani, K. W. Jolley, D. L. Officer, P. J. Walsh, K. Gordon, R. Humphry-Baker, M. K. Nazeeruddin, M. Graetzel, *J. Phys. Chem. B* **2005**, *109*, 15397-15409.

[6] a) J. A. S. Cavaleiro, A. C. Tome, M. G. P. M. S. Neves, *Handbook of Porphyrin Science* **2010**, *2*, 193-294; b) N. N. Sergeeva, M. O. Senge, A. Ryan, *Handbook of Porphyrin Science* **2010**, *3*, 325-365.

[7] R. Deshpande, L. Jiang, G. Schmidt, J. Rakovan, X. Wang, K. Wheeler, H. Wang, *Org. Lett.* **2009**, *11*, 4251-4253.

[8] A. K. Burrell, D. L. Officer, *Synlett* **1998**, *1998*, 1297-1307.

[9] a) W. M. Campbell, K. W. Jolley, P. Wagner, K. Wagner, P. J. Walsh, K. C. Gordon, L. Schmidt-Mende, M. K. Nazeeruddin, Q. Wang, M. Gratzel, D. L. Officer, *J. Phys. Chem. C* **2007**, *111*, 11760-11762; b) K. Dahms, M. O. Senge, M. B. Bakar, *Eur. J. Org. Chem.* **2007**, *2007*, 3833-3848.

[10] W. J. Belcher, A. K. Burrell, D. L. Officer, D. C. W. Reid, S. M. Scott, *J. Porphyrins Phthalocyanines* **2002**, *6*, 720-736.

[11] E. E. Bonfantini, A. K. Burrell, D. L. Officer, D. C. W. Reid, M. R. McDonald, P. A. Cocks, K. C. Gordon, *Inorg. Chem.* **1997**, *36*, 6270-6278.

[12] K. M. Kadish, E. Van Caemelbecke, G. Royal, in *The Porphyrin Handbook* (Eds.: K. M. Kadish, K. M. Smith, R. Guilard), Academic Press, San Diego, **2000**, pp. 1-114.

[13] A. K. Burrell, D. L. Officer, D. C. W. Reid, S. M. Scott, K. C. Gordon, *J. Porphyrins Phthalocyanines* **2000**, *4*, 626-633.

[14] a) H. L. Anderson, *Inorg. Chem.* **1994**, *33*, 972-981; b) V. Lin, S. DiMagno, M. Therien, *Science* **1994**, *264*, 1105-1111.

[15] M. Gouterman, *J. Chem. Phys.* **1959**, *30*, 1139-1161.

[16] a) S. Choi, T. G. Spiro, *J. Am. Chem. Soc.* **1983**, *105*, 3683-3692; b) N. Parthasarathi, C. Hansen, S. Yamaguchi, T. G. Spiro, *J. Am. Chem. Soc.* **1987**, *109*, 3865-3871; c) G. S. S. Saini, S. Dogra, G. Singh, S. K. Tripathi, S. Kaur, V. Sathe, B. C. Choudhary, *Vib. Spectrosc.* **2012**, *61*, 188-198; d) L. D. Sparks, K. K. Anderson, C. J. Medforth, K. M. Smith, J. A. Shelnutt, *Inorg. Chem.* **1994**, *33*, 2297-2302.

[17] R. Horvath, K. C. Gordon, *Coord. Chem. Rev.* **2010**, *254*, 2505-2518.

[18] M. Gouterman, G. H. Wagnière, L. C. Snyder, *J. Mol. Spectrosc.* **1963**, *11*, 108-127.

[19] Z. Denden, K. Ezzayani, E. Saint‐Aman, F. Loiseau, S. Najmudin, C. Bonifácio, J. C. Daran, H. Nasri, *Eur. J. Inorg. Chem.* **2015**, *2015*, 2596-2610.

[20] J. C. Earles, K. C. Gordon, A. W. I. Stephenson, A. C. Partridge, D. L. Officer, *Phys. Chem. Chem. Phys.* **2011**, *13*, 1597-1605.

[21] H. van der Salm, P. Wagner, K. Wagner, D. L. Officer, G. G. Wallace, K. C. Gordon, *Chem. - Eur. J.* **2015**, *21*, 15622-15632.

[22] R. P. Ortiz, S. R. Gonzalez, J. Casado, J. T. Lopez Navarrete, D. L. Officer, P. Wagner, J. C. Earles, K. C. Gordon, *ChemPhysChem* **2009**, *10*, 1901-1910.

[23] M. Urbani, M. Grätzel, M. K. Nazeeruddin, T. Torres, *Chem. Rev.* **2014**, *114*, 12330-12396.

[24] T. Dos Santos, A. Morandeira, S. Koops, A. J. Mozer, G. Tsekouras, Y. Dong, P. Wagner, G. Wallace, J. C. Earles, K. C. Gordon, D. Officer, J. R. Durrant, *J. Phys. Chem. C* **2010**, *114*, 3276-3279.

[25] P. Leighton, J. A. Cowan, R. J. Abraham, J. K. M. Sanders, *J. Org. Chem.* **1988**, *53*, 733-740.

Entry for the Table of Contents

FULL PAPER

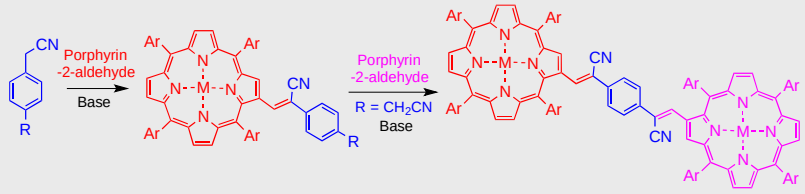

β-Vinyl substituted porphyrins and porphyrin dyads are readily synthesized using Knoevenagel condensations, with the efficacy of this type of porphyrin dye determined in a dye sensitised solar cell.

Porphyrins

Rhys Mitchell, Klaudia Wagner, Jonathan Barnsley, Holly van der Salm, Keith C. Gordon, David L. Officer and Pawel Wagner**

Page No. – Page No.

Synthesis and Light Harvesting Potential of Cyanovinyl β-Substituted Porphyrins and Dyads